activate both tumor antigen-specific $CD8^+$ CTLs at the tumor implanted site and NK cells in metastatic regions at the same time even in the absence of externally added tumor antigens. Activated DEC-205^+ DCs may take up tumor antigens from tumor cells and cross-present tumor-derived epitopes in association with class I MHC molecules of their own to prime epitope-specific $CD8^+$ CTLs in vivo that can attack already established tumors. Although the precise mechanism remains to be investigated, such selectively stimulated DEC-205^+ DCs appear also to activate NK cells that prevent tumor metastasis. Indeed, very recently, Sancho et al. [9] reported the usefulness of targeting DEC-205^+ DCs with DNGR-1.

We have not confirmed the actual effector cells involved in the regression of the implanted tumors such as Hepa1-6 hepatoma and B16-F10 melanoma cells, on which down-modulated class I MHC molecules are sometimes expressed, and thus they might be targets for activated NK cells. Therefore, in order to confirm whether the cells involved in tumor regression are actually class I MHC molecule-restricted epitope-specific conventional $CD8^+$ CTLs in this system, we conducted similar experiments using syngeneic E.G7-OVA and B16-OVA tumor cells that should be eliminated by $CD8^+$ CTLs recognizing the known CTL epitope (SIINFEKL) presented by K^b class I MHC molecules rather than by NK cells. In comparison with other syngeneic tumors, the regression of implanted E.G7-OVA in $33D1^+$ DC-deleted mice was almost unchanged by two injections of LPS. Nevertheless, ip inoculation of a mouse with L-PAM at a very low unaffected dose 10 days after implantation of E.G7-OVA resulted in marked reduction of the implanted EG7-OVA. In regressed tumors, we have observed an increased number of $CD8^+$ H-2 K^b/OVA tetramer-positive cells showing marked epitope-specific cytotoxic activities. These results indicate that selective stimulation of DEC-205^+ DCs in vivo may generate acquired epitope-specific class I MHC molecule-restricted conventional $CD8^+$ CTLs against already established tumors, such as E.G7-OVA expressing class I MHC when they are slightly attacked with a very small amount of anticancer drugs, such as L-PAM. However, as shown with B16-OVA, selective stimulation of innate DEC-205^+ DCs appears superior for controlling cancer drug-resistant tumors instead of a high dose of anticancer drugs.

Taken together, the findings of the present study suggest the importance and effectiveness of selective targeting of a specific subset of innate DCs, such as DEC-205^+ DCs, together with very small doses of anticancer drugs against established tumors to activate functional acquired MHC-I-associated effectors, such as both $CD8^+$ CTLs and NK cells in vivo without co-administration of tumor epitope antigens and provide a new direction for tumor immunotherapy.

Acknowledgments This work was supported in part by Grants from the Ministry of Education, Science, Sport, and Culture, from the Ministry of Health and Labor and Welfare, Japan, and from the Japanese Health Sciences Foundation, and by the Promotion and Mutual Aid Corporation for Private Schools of Japan.

References

1. Takahashi H, Nakagawa Y, Yokomuro K, Berzofsky JA (1993) Induction of $CD8^+$ cytotoxic T lymphocytes by immunization with syngeneic irradiated HIV-1 envelope derived peptide-pulsed dendritic cells. Int Immunol 5(8):849–857
2. Takahashi H (2003) Antigen presentation in vaccine development. Comp Immunol Microbiol Infect Dis 26(5–6):309–328
3. Bevan MJ (1976) Cross-priming for a secondary cytotoxic response to minor h antigens with H-2 congenic cells which do not cross-react in the cytotoxic assay. J Exp Med 143(5):1283–1288
4. Melief CJ (2003) Mini-review: regulation of cytotoxic T lymphocyte responses by dendritic cells: peaceful coexistence of cross-priming and direct priming? Eur J Immunol 33(10):2645–2654
5. Takahashi H, Takeshita T, Morein B, Putney S, Germain RN, Berzofsky JA (1990) Induction of $CD8^+$ cytotoxic T cells by immunization with purified HIV-1 envelope protein in ISCOMs. Nature 344(6269):873–875
6. Fujimoto C, Nakagawa Y, Ohara K, Takahashi H (2004) Polyriboinosinic polyribocytidylic acid [poly(i:C)]/TLR3 signaling allows class I processing of exogenous protein and induction of HIV-specific $CD8^+$ cytotoxic T lymphocytes. Int Immunol 16(1):55–63
7. Dudziak D, Kamphorst AO, Heidkamp GF, Buchholz VR, Trumpfheller C, Yamazaki S, Cheong C, Liu K, Lee HW, Park CG, Steinman RM, Nussenzweig MC (2007) Differential antigen processing by dendritic cell subsets in vivo. Science 315(5808):107–111
8. Trumpfheller C, Caskey M, Nchinda G, Longhi MP, Mizenina O, Huang Y, Schlesinger SJ, Colonna M, Steinman RM (2008) The microbial mimic poly ic induces durable and protective $CD4^+$ T cell immunity together with a dendritic cell targeted vaccine. Proc Natl Acad Sci U S A 105(7):2574–2579
9. Sancho D, Mourao-Sa D, Joffre OP, Schulz O, Rogers NC, Pennington DJ, Carlyle JR, Reis e Sousa C (2008) Tumor therapy in mice via antigen targeting to a novel, DC-restricted C-type lectin. J Clin Invest 118(6):2098–2110
10. Fernandez NC, Lozier A, Flament C, Ricciardi-Castagnoli P, Bellet D, Suter M, Perricaudet M, Tursz T, Maraskovsky E, Zitvogel L (1999) Dendritic cells directly trigger NK cell functions: cross-talk relevant in innate anti-tumor immune responses in vivo. Nat Med 5(4):405–411
11. Wakabayashi A, Nakagawa Y, Shimizu M, Moriya K, Nishiyama Y, Takahashi H (2008) Suppression of an already established tumor growing through activated mucosal CTLs induced by oral administration of tumor antigen with cholera toxin. J Immunol 180(6):4000–4010
12. Rowe DS, Fahey JL (1965) A new class of human immunoglobulins. I. A unique myeloma protein. J Exp Med 121:171–184
13. Wang X, Fjerdingstad H, Strom-Gundersen I, Benestad HB (1999) Maturation rate of mouse neutrophilic granulocytes: acceleration by retardation of proliferation, but no detectable influence from G-CSF or stromal cells. Stem Cells 17(5):253–264

14. Calder CJ, Liversidge J, Dick AD (2004) Murine respiratory tract dendritic cells: Isolation, phenotyping and functional studies. J Immunol Methods 287(1–2):67–77
15. Takahashi H, Nakagawa Y, Leggatt GR, Ishida Y, Saito T, Yokomuro K, Berzofsky JA (1996) Inactivation of human immunodeficiency virus (HIV)-1 envelope-specific $CD8^+$ cytotoxic T lymphocytes by free antigenic peptide: a self-veto mechanism? J Exp Med 183(3):879–889
16. Rotzschke O, Falk K, Stevanovic S, Jung G, Walden P, Rammensee HG (1991) Exact prediction of a natural T cell epitope. Eur J Immunol 21(11):2891–2894
17. Nakatsuka K, Sugiyama H, Nakagawa Y, Takahashi H (1999) Purification of antigenic peptide from murine hepatoma cells recognized by class-I major histocompatibility complex molecule-restricted cytotoxic T-lymphocytes induced with B7-1-gene-transfected hepatoma cells. J Hepatol 30(6):1119–1129
18. Ben-Efraim S, Bocian RC, Mokyr MB, Dray S (1983) Increase in the effectiveness of melphalan therapy with progression of MOPC-315 plasmacytoma tumor growth. Cancer Immunol Immunother 15(2):101–107
19. Takesue BY, Pyle JM, Mokyr MB (1990) Importance of tumor-specific cytotoxic $CD8^+$ T-cells in eradication of a large subcutaneous MOPC-315 tumor following low-dose melphalan therapy. Cancer Res 50(23):7641–7649
20. Pack M, Trumpfheller C, Thomas D, Park CG, Granelli-Piperno A, Munz C, Steinman RM (2008) Dec-205/$CD205^+$ dendritic cells are abundant in the white pulp of the human spleen, including the border region between the red and white pulp. Immunology 123(3):438–446
21. van den Broeke LT, Daschbach E, Thomas EK, Andringa G, Berzofsky JA (2003) Dendritic cell-induced activation of adaptive and innate antitumor immunity. J Immunol 171(11):5842–5852
22. Peron JM, Esche C, Subbotin VM, Maliszewski C, Lotze MT, Shurin MR (1998) Flt3-ligand administration inhibits liver metastases: role of NK cells. J Immunol 161(11):6164–6170

Interferon-γ and tumor necrosis factor-α induce an immunoinhibitory molecule, B7-H1, via nuclear factor-κB activation in blasts in myelodysplastic syndromes

Asaka Kondo,[1] Taishi Yamashita,[1,2] Hideto Tamura,[1] Wanhong Zhao,[1] Takashi Tsuji,[2] Masumi Shimizu,[3] Eiji Shinya,[3] Hidemi Takahashi,[3] Koji Tamada,[4] Lieping Chen,[5] Kazuo Dan,[1] and Kiyoyuki Ogata[1]

[1]Division of Hematology, Department of Medicine, Nippon Medical School, Tokyo, Japan; [2]Department of Biological Science and Technology, Tokyo University of Science, Chiba, Japan; [3]Department of Microbiology and Immunology, Nippon Medical School, Tokyo, Japan; [4]Department of Otorhinolaryngology–Head and Neck Surgery, Marlene and Stewart Greenebaum Cancer Center, University of Maryland, Baltimore; and [5]Department of Oncology, Johns Hopkins University School of Medicine, Baltimore, MD

During disease progression in myelodysplastic syndromes (MDS), clonal blasts gain a more aggressive nature, whereas nonclonal immune cells become less efficient via an unknown mechanism. Using MDS cell lines and patient samples, we showed that the expression of an immunoinhibitory molecule, B7-H1 (CD274), was induced by interferon-γ (IFNγ) and tumor necrosis factor-α (TNFα) on MDS blasts. This induction was associated with the activation of nuclear factor-κB (NF-κB) and nearly completely blocked by an NF-κB inhibitor, pyrrolidine dithiocarbamate (PDTC). B7-H1$^+$ MDS blasts had greater intrinsic proliferative capacity than B7-H1$^-$ MDS blasts when examined in various assays. Furthermore, B7-H1$^+$ blasts suppressed T-cell proliferation and induced T-cell apoptosis in allogeneic cocultures. When fresh bone marrow samples from patients were examined, blasts from high-risk MDS patients expressed B7-H1 molecules more often compared with those from low-risk MDS patients. Moreover, MDS T cells often overexpressed programmed cell death 1 (PD-1) molecules that transmit an inhibitory signal from B7-H1 molecules. Taken together, these findings provide new insight into MDS pathophysiology. IFNγ and TNFα activate NF-κB that in turn induces B7-H1 expression on MDS blasts. B7-H1$^+$ MDS blasts have an intrinsic proliferative advantage and induce T-cell suppression, which may be associated with disease progression in MDS. (*Blood*. 2010;116(7):1124-1131)

Introduction

B7-H1 (CD274), which was identified by us as a costimulatory molecule, plays a crucial role in T-cell regulation in various immune responses.[1,2] B7-H1 molecules deliver a costimulatory signal through an unknown receptor on naive T cells.[1-3] They also deliver an inhibitory signal to activated T cells through programmed cell death 1 (PD-1) molecules,[4] which are a type I transmembrane protein belonging to the CD28 receptor family and were originally identified in T cells undergoing apoptosis.[5] B7-H1 expression is detected not only on antigen-presenting cells but also on activated T cells and some tumor cells (ie, renal cell, colon, breast, and lung carcinoma, and Hodgkin lymphoma).[6-10] Rodent data suggest that B7-H1 molecules on tumor cells deliver negative signals through PD-1 and other receptors on tumor-specific cytotoxic T lymphocytes and inhibit antitumor immune responses.[11,12] Consistent with those data, it was reported that in patients with renal cell carcinoma and breast cancer, patients whose tumor cells expressed B7-H1 had a poor prognosis.[9,13] In a mouse leukemia model in which mice were immunized with irradiated DA1-3b leukemia cells and then challenged with live DA1-3b cells, only leukemia cells expressing high levels of B7-H1 survived for a long period. Moreover, these cells gained tolerance to specific cytotoxic T lymphocyte–mediated killing.[14] Therefore, B7-H1 molecules on leukemia cells may be associated with immune evasion in this model.

Myelodysplastic syndromes (MDS) are clonal hematologic stem cell disorders characterized by cytopenias, excessive apoptosis of hematopoietic cells, and a high risk of progression to acute myeloid leukemia (AML). In MDS, various immune abnormalities, including lymphopenia and T-cell dysfunction, have been reported,[15-17] although data on B7-related molecules, in particular B7-H1, are lacking. With disease progression, that is, with increases in blast percentages in the bone marrow (BM), clonal MDS blasts become less apoptotic, more proliferative, and phenotypically more immature,[18,19] whereas nonclonal immune cells become less efficient with a decrease in T-cell number and increases in T-cell apoptosis and in the number of CD4$^+$ regulatory T cells.[16,20,21] However, the mechanism for these observed phenomena linked to disease progression is largely unknown. It is also notable that in a recent study in which MDS patients were treated with the immunomodulatory drug lenalidomide,[22] the results suggested that appropriate immunomodulation is effective in suppressing/eradicating MDS clones at least in some cases.[23] In the present study, we investigated whether B7-H1 molecules are expressed on MDS blasts, and if so, whether they are associated with the pathophysiology of MDS.

Methods

Cell lines and patients

F-36P, OIH-1 (Riken Cell Bank, Ibaraki, Japan), and SKM-1 (Health Science Research Resources Bank, Osaka, Japan) cells, which are appropriate among the limited number of MDS-related cell lines,[24] have a blast morphology, and have been established from AML patients transformed

Submitted November 27, 2009; accepted April 22, 2010. Prepublished online as *Blood* First Edition paper, May 14, 2010; DOI 10.1182/blood-2009-12-255125.

The online version of this article contains a data supplement.

The publication costs of this article were defrayed in part by page charge payment. Therefore, and solely to indicate this fact, this article is hereby marked "advertisement" in accordance with 18 USC section 1734.

Table 1. Patient characteristics for study comparing blasts in MDS

Characteristic	No. of patients
Sex, M/F	35/26
Median age, y (range)	70 (32-88)
World Health Organization subtype	
RCUD	9
RCMD	6
RAEB-1	5
RAEB-2	9
AL-MDS	32
IPSS category*	
Low	6
Intermediate-1	9
Intermediate-2	10
High	15
Unknown	1

MDS indicates myelodysplastic syndromes; RCUD, refractory cytopenia with unilineage dysplasia; RCMD, refractory cytopenia with multilineage dysplasia; RAEB, refractory anemia with excess blasts; AL-MDS, acute myeloid leukemia transformed from MDS; and IPSS, International Prognostic Scoring System.

*Not applicable for patients whose bone marrow contained 30% or more blasts.

from MDS (AL-MDS), were cultured in RPMI 1640 medium containing 10% fetal bovine serum, and L-glutamine 1mM. Interleukin-3 (IL-3; 5 ng/mL; Peprotech) and granulocyte colony–stimulating factor (5 ng/mL; Peprotech) were added to the F-36P and OIH-1 cultures, respectively, according to the instructions of the suppliers. The RPMI 1640 medium with or without IL-3 or granulocyte colony–stimulating factor is simply referred to as "the medium" in the present experiments. Because OIH-1 cells are often difficult to maintain, we used F-36P and SKM-1 cells for most experiments.

Portions of BM cells aspirated from subjects for diagnostic purposes were used after receiving written informed consent. The study participants included 29 MDS patients, 32 AL-MDS patients in whom a history of MDS was confirmed, and 10 hematologically normal subjects (Table 1). The patients were diagnosed according to the World Health Organization classification.[25] Patients with secondary MDS and those who had had infections within 1 month before this study were excluded. Karyotypes were analyzed using the standard G-banding technique. Patients were classified according to the International Prognostic Scoring System (IPSS) as described previously.[26] Peripheral blood (PB) was sampled to examine PD-1 expression on T cells. Mononuclear cells (MNCs) separated from BM and PB samples with Histopaque (Sigma-Aldrich) density centrifugation were also used in experiments.

To induce B7-H1 expression, the cells were cultured in the presence of the human cytokines interferon-γ (IFNγ; 1000 U/mL; Peprotech), IL-1β (10 ng/mL; Peprotech), transforming growth factor-β (TGFβ, 10 ng/mL; Peprotech), and tumor necrosis factor-α (TNFα; 500 U/mL; Peprotech) for 2 days. An inhibitor of nuclear factor-κB (NF-κB), pyrrolidine dithiocarbamate (PDTC; Sigma-Aldrich), was added to cultures in some experiments. In some experiments, B7-H1$^+$ and B7-H1$^-$ blasts from patient samples or cell lines and CD34$^+$ cells from patient samples were purified using fluorescence-activated cell sorting (FACS) as described previously.[27]

This study protocol was approved by the Institutional Review Board of Nippon Medical School.

Reverse-transcription polymerase chain reaction

Total cellular RNA was extracted from exponentially growing cell lines and reverse-transcribed with Superscript II Reverse transcriptase (Invitrogen) using random hexamers. The success of cDNA synthesis was monitored by the reverse-transcription polymerase chain reaction (PCR) of β-actin. PCR synthesis using primers for B7-H1 was performed as described previously.[28]

In some experiments, purified B7-H1$^+$ and B7-H1$^-$ F-36P cells were used for the RNA source and their *cyclin D1*, *D2*, *D3*, *E1*, and *E2* gene expressions were examined using real-time quantitative PCR as described previously.[27] Their primers are shown in supplemental Table 1 (available on the *Blood* Web site; see the Supplemental Materials link at the top of the online article).

B7-H1 and PD-1 flow cytometric analyses

All antibodies used in this study were mouse anti–human monoclonal antibodies. B7-H1 expression on MDS cell lines and BM blasts from subjects as well as PD-1 expression on circulating T cells were determined using flow cytometry (FCM), as described previously.[16,29] MDS cell lines were stained with anti–B7-H1–phycoerythrin (PE; eBioscience). The BM MNCs were stained with anti-CD45–peridin chlorophyll (PerCP), anti-CD34–fluorescein isothiocyanate (FITC; BD Biosciences), and anti–B7-H1–PE. In MDS patients, blasts were gated using the CD45-gating method and the gating was confirmed by CD34-positivity of the gated blasts. In some cases, the gated blasts were isolated using FACS, and it was confirmed that they were actual blasts. Because blasts from hematologically normal subjects were often too few to gate correctly, B7-H1 expression was examined on CD34$^+$ myeloblasts, which were identified according to the gating method described in detail previously.[29] PB MNCs were stained with anti–PD-1–FITC (eBioscience) and either PE-conjugated anti-CD3, -CD4, or -CD8 (BD Biosciences) or, in some cases, with anti–PD-1–FITC, anti–HLA-DR-PE (Beckman Coulter), and anti-CD3–PerCP. Single-labeled cells were used to compensate for the fluorescence emission overlap of each fluorochrome into inappropriate channels. Isotype-matched negative controls were used in all assays.

Immunocytochemistry for NF-κB p65 localization

The nuclear translocation of NF-κB p65 (ie, the activation of NF-κB) was examined using the immunocytochemical method.[30] Briefly, cells fixed with paraformaldehyde were plated on a poly-L-lysine–coated glass slide, air-dried, and treated with 0.2% Triton X-100. After washing in phosphate-buffered saline, slides were blocked with 5% normal goat serum for 1 hour and then incubated with rabbit polyclonal anti–human p65 antibody (Cell Signaling Technology) at 1:100 dilution. After overnight incubation at 4°C, the slides were washed and incubated with goat anti–rabbit immunoglobulin G (IgG)–Alexa Fluor 594 at 1:100 dilution for 1 hour. Stained slides were mounted with mounting medium containing 4′-6-diamidino-2-phenylindole for nuclear staining (Vector Laboratories) and analyzed under a fluorescence microscope (IX71; Olympus). Images were acquired and analyzed with Aquacosmos software (Hamamatsu Photonics).

Western blot analysis of NF-κB p65 translocation

Extracts from the cytoplasmic and nuclear fractions of cells were prepared with the Lysate Preparation Module (IMGENEX). Equal amounts of extracts (corresponding to 1×10^5 cells) from each fraction were separated on 10% sodium dodecyl sulfate–polyacrylamide gel electrophoresis and transferred to a polyvinylidene difluoride membrane. The blots were probed with a monoclonal antibody for p65 (Cell Signaling Technology) and detected using an ECL Plus detection kit (GE Healthcare) with horseradish peroxidase-conjugated anti–rabbit IgG (Cell Signaling Technology). Band intensity was quantified with the use of Scion Image software (Scion Corporation).

Cell-cycle, bromodeoxyuridine, and Ki-67 analyses, colony-forming assay, and apoptosis analysis

For cell-cycle analysis, cells were stained with unlabeled anti–B7-H1 antibody (eBioscience) and then with anti–mouse IgG-FITC. After washing, the cells were fixed in 70% cold ethanol, washed, and resuspended in 100 μL of phosphate-buffered saline containing 1 μL of RNase and 0.1 mg/mL propidium iodide (PI; Sigma-Aldrich). The cell cycle of B7-H1$^+$ and B7-H1$^-$ cells was determined using FCM.[31]

For bromodeoxyuridine (BrdU) analysis, cells were pulsed with BrdU (BrdU flow kit; BD Biosciences) at a concentration of 10μM for 1 hour, washed, and stained with anti–B7-H1–PE. Then, cells were permeabilized and labeled with anti-BrdU–FITC according to the manufacturer's instructions. For Ki-67 analysis, cells were stained with anti–B7-H1–PE and

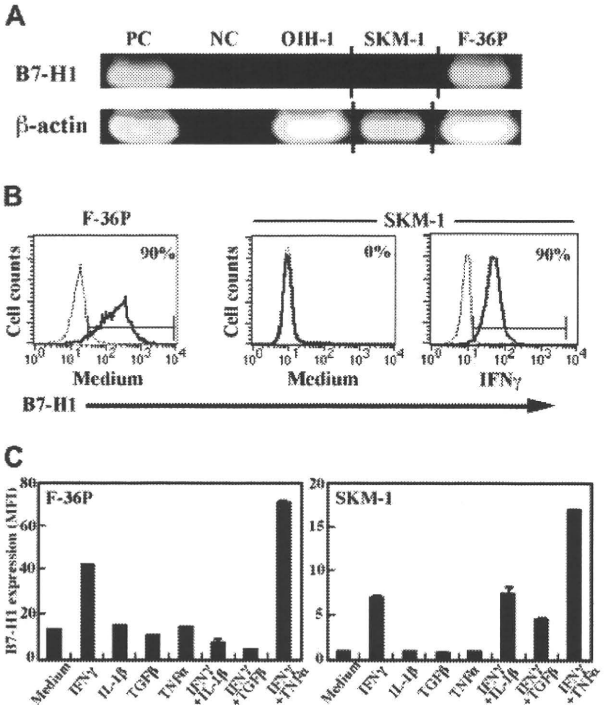

Figure 1. Constitutive or inducible B7-H1 expression in MDS cell lines. (A) *B7-H1* mRNA expression analyzed by reverse-transcription polymerase chain reaction. Equal amounts of cDNA from 3 myelodysplastic syndromes (MDS) cell lines were amplified. Vertical lines have been inserted to indicate a repositioned gel lane. (B) B7-H1 expression analyzed by flow cytometry (FCM). The cell lines were cultured with medium alone or with IFNγ. Thick line histogram represents staining with anti–B7-H1 monoclonal antibodies; dotted line histogram represents staining with isotype-matched control Ig. (C) Effects of cytokines on B7-H1 expression in F-36P and SKM-1 cells. Data (relative fluorescence intensity [MFI]) are mean and SD of 3 experiments. Results without SD error bar indicate small SD.

anti-CD45–PerCP, washed, permeabilized with 75% ethanol, and stained with anti–Ki-67–FITC (FITC mouse anti–human Ki-67 set; BD Biosciences) according to the manufacturer's instructions.

The colony-forming activity of purified B7-H1$^+$ and B7-H1$^-$ F-36P cells was examined after culturing in MethoCult H4230 methylcellulose medium (StemCell Technologies) supplemented with IL-3 (10 ng/mL). Colonies (aggregates of 50 cells or more) were scored on day 7 of culture.

For apoptosis analysis, the cells were stained with one of the PE-conjugated antibodies to CD3, CD4, or CD8 and with annexin V–FITC and PI (Trevigen), according to the manufacturer's instructions, and then analyzed using FCM.[16] In some experiments, B7-H1$^+$ and B7-H1$^-$ F-36P cells prepared after labeling with anti–B7-H1–PE were cultured with lymphocytes. In this case, the cells were stained with anti-CD3–allophycocyanin (BD Biosciences) and with annexin V–FITC and PI. For caspase-3 analysis, the cells were first stained with FITC-conjugated antibodies to CD3, CD4, or CD8, washed, and then stained for the active form of caspase-3 using an FCM kit (BD Biosciences).

Mixed lymphocyte–blast reaction

CD3$^+$, CD4$^+$, and CD8$^+$ T cells were purified from PB from healthy volunteers using magnetic cell sorting (Miltenyi Biotec). The purity of the isolated cells was more than 95% as determined in FCM. Each of these cell populations (1×10^5 cells/well) was cocultured with irradiated (20 000 rad) MDS blasts, that is, either F-36P cells (whole cells or purified cells according to the status of B7-H1 expression) or patient blasts that were confirmed to express B7-H1, in 96-well U-bottomed plates for 5 days. Antagonistic anti–B7-H1 (eBioscience) or anti–PD-1 (R&D Systems) antibody was added to the culture to block the B7-H1–PD-1 pathway. These mixed lymphocyte–blast reaction (MLR) cultures were subjected to 2 types of assay. To determine T-cell proliferation, ^{3}H-thymidine (1 μCi/well) was added to the wells during the last 18 hours of culture, and its incorporation into T cells was measured. To determine T-cell apoptosis, the cells were subjected to apoptosis analysis after 5-day MLR culture.

Morphometric analysis

Cytospin preparations were prepared using B7-H1$^+$ and B7-H1$^-$ blasts isolated by FACS and stained with Wright-Giemsa. Their images were captured with an Olympus AX-80 microscope connected to a digital camera (DP50; Olympus), and diameters of the nucleus and cytoplasm were measured using analysis software (Lumina Vision; Mitani Corportion). One

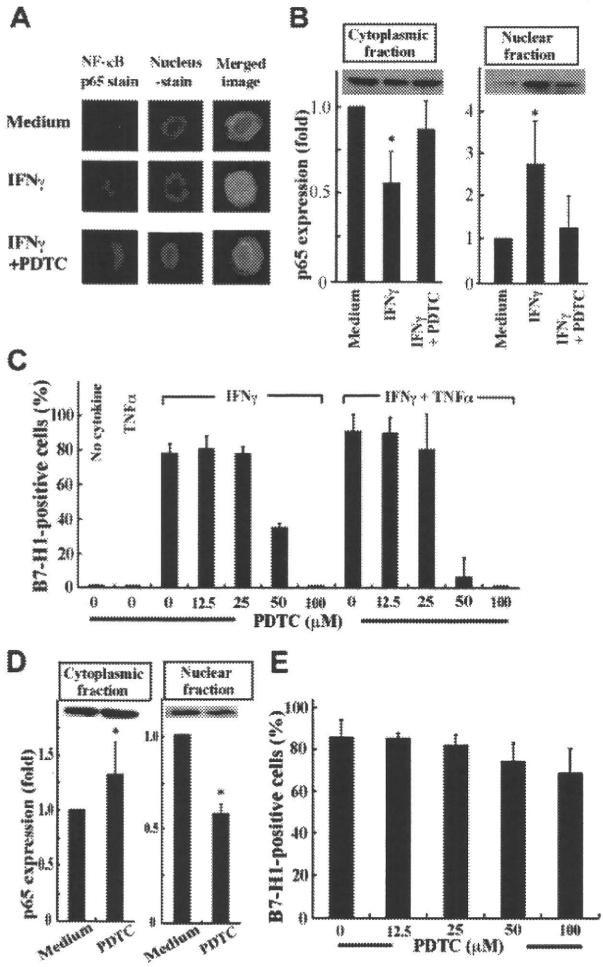

Figure 2. Inhibition of NF-κB activation down-regulated B7-H1 expression. (A) SKM-1 cells cultured for 24 hours with medium alone, IFNγ, or IFNγ and pyrrolidine dithiocarbamate (PDTC; 100μM) were stained for NF-κB p65 (red) and nuclei (blue). The merged image showed that IFNγ induced p65 localization into the nucleus, which was inhibited by PDTC. Images were acquired on an Olympus IX71 inverted microscope using a LCPlanFl 40×/0.60 objective lens. Alexa 594 and 4′-6-diamidino-2-phenylindole were detected using Fluorescence Miler Units of U-MWIG2 and U-MNUA2 (Olympus), respectively. Images were captured using a 3CCD digital color camera (Hamamatsu Photonics) through Aquacosmos Software. (B) After the cultures in A, SKM-1 cells were separated into cytoplasmic and nuclear fractions, and their p65 contents were analyzed by Western blotting to show representative (top panel) and quantified (bottom panel) data (mean + SD) of 3 experiments. In each experiment, the band intensity of cell fractions from SKM-1 cells cultured with medium alone was defined as 1. *P = .017 and .06 (left panel) and *P = .045 and .012 (right panel) compared with "the medium" and IFNγ and PDTC, respectively. (C) SKM-1 cells cultured with or without cytokine(s) and various concentrations of PDTC were analyzed for B7-H1 expression by FCM. (D-E) Using F-36P cells expressing B7-H1 constitutively, the same experiments as in panels B and C were performed, except that no cytokines were used. Data are from 3 experiments. *P = .015 for D (left panel) and *P < .0001 (right panel) compared with the medium.

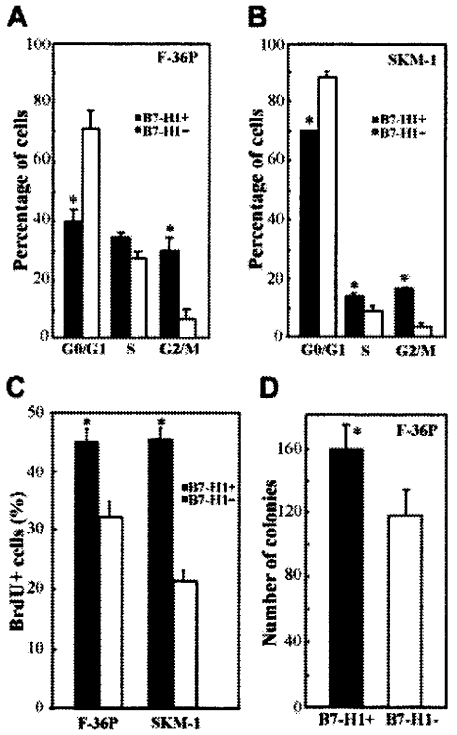

Figure 3. Cell proliferative potential as a function of B7-H1 expression in MDS cell lines. (A-B) Cell-cycle analysis of B7-H1$^+$ and B7-H1$^-$ cell fractions in F-36P (A) and SKM-1 (B) cells. SKM-1 cells were cultured with IFNγ for 2 days before analyses. (C) BrdU incorporation in B7-H1$^+$ and B7-H1$^-$ cell fractions in F-36P and SKM-1 cells. (D) The number of colonies formed by purified B7-H1$^+$ and B7-H1$^-$ F-36P cells in the methylcellulose culture. Data in panels A through C are mean (and SD) of 3 experiments. *$P < .036$ for B7-H1$^+$ versus B7-H1$^-$ cell fractions.

hundred cells were analyzed for each cell fraction. Forward and side light scatter values in FCM for B7-H1$^+$ and B7-H1$^-$ blasts, which reflect cell size and cytoplasmic granularity, respectively, were also analyzed. Only samples in which data on more than 100 events were available for both blast populations were used for analysis.

Statistical analysis

Differences between 2 groups of data were determined using Student *t* test for continuous variables and the χ^2 test for categorical variables. A *P* value less than .05 was considered to represent a statistically significant difference.

Results

B7-H1 expression in MDS cell lines

First, the expression of B7-H1 molecules was examined in 3 MDS cell lines cultured without any specific stimulation of B7-H1 (Figure 1A,B left and middle panels). A high level of B7-H1 expression at the mRNA and protein levels was detected in F-36P cells. OIH-1 and SKM-1 cells expressed less and an undetectable amount of *B7-H1* mRNA, respectively, and B7-H1 protein was not detectable on their cell surface. Next, we investigated whether cytokines that may be associated with MDS pathophysiology (ie, IFNγ, IL-1β, TGFβ, and TNFα) induced B7-H1 expression in these cells. IFNγ, which is known to induce B7-H1 expression in antigen-presenting cells from healthy subjects, enhanced or induced B7-H1 expression in all 3 cell lines (right panels of Figure 1B-C). Notably, the combination of IFNγ and TNFα induced a much higher level of B7-H1 expression than IFNγ alone in the F-36P and SKM-1 cell lines.

Involvement of NF-κB activation in B7-H1 induction in MDS cells

IFNγ and TNFα activate NF-κB in human cells,[32-34] and the promoter region of the human B7-H1 gene has an NF-κB motif.[35] NF-κB activation was also observed in MDS patients, in particular in patients with advanced disease.[36,37] Therefore, we next investigated whether B7-H1 induction by IFNγ and TNFα in MDS cells is mediated by NF-κB activation. When SKM-1 cells were treated with IFNγ, the nuclear translocation of NF-κB p65, indicating NF-κB activation, was observed, and was nearly completely blocked by the NF-κB inhibitor, PDTC (Figure 2A-B). Furthermore, B7-H1 induction by IFNγ and TNFα in SKM-1 cells was completely blocked by PDTC (Figure 2C). When F-36P cells that constitutively express B7-H1 molecules were examined, NF-κB was also constitutively activated (strong Western blot band in the nuclear fraction; Figure 2D). When using PDTC, NF-κB activation and B7-H1 expression were partially inhibited in F-36P cells (Figure 2D-E).

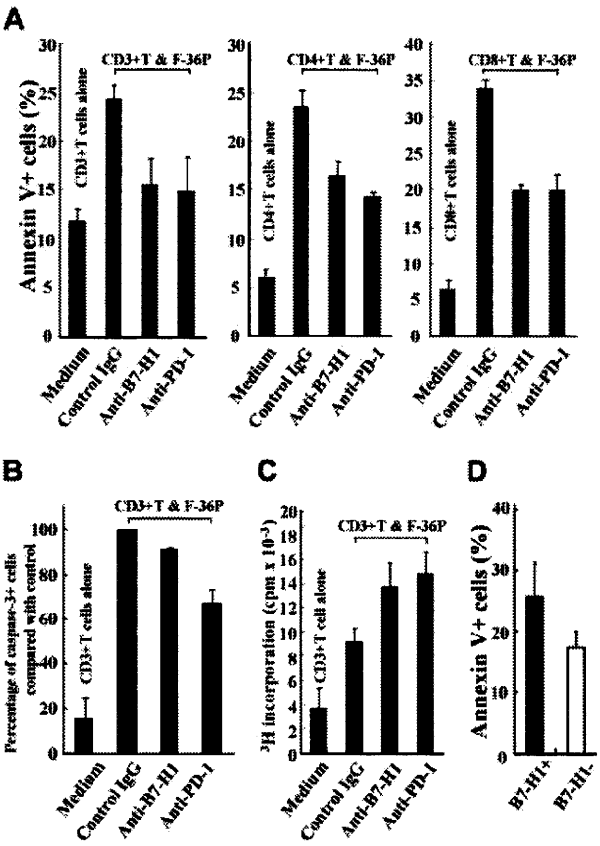

Figure 4. Effects of B7-H1 molecules expressed by blasts on T cells. (A-C) Purified, normal CD3$^+$, CD4$^+$, and CD8$^+$ T cells were cultured alone or with irradiated F-36P cells in the presence of either control immunoglobulin G (IgG), anti–B7-H1 monoclonal antibody, or anti–PD-1 monoclonal antibody. Data are mean (and SD) of 3 experiments. $P < .05$ when data in each of the 2 columns on the right were compared with control IgG data. (A) The percentage of annexin V$^+$ cells in each T-cell fraction. (B) The percentage of caspase-3$^+$ cells in T cells. Data labeled control IgG were defined as 100% in each experiment. (C) T-cell proliferation determined in the ^{3}H-thymidine incorporation assay. (D) Normal CD3$^+$ T cells were cultured with irradiated F-36P cells that had been purified into either B7-H1$^+$ or B7-H1$^-$ cells.

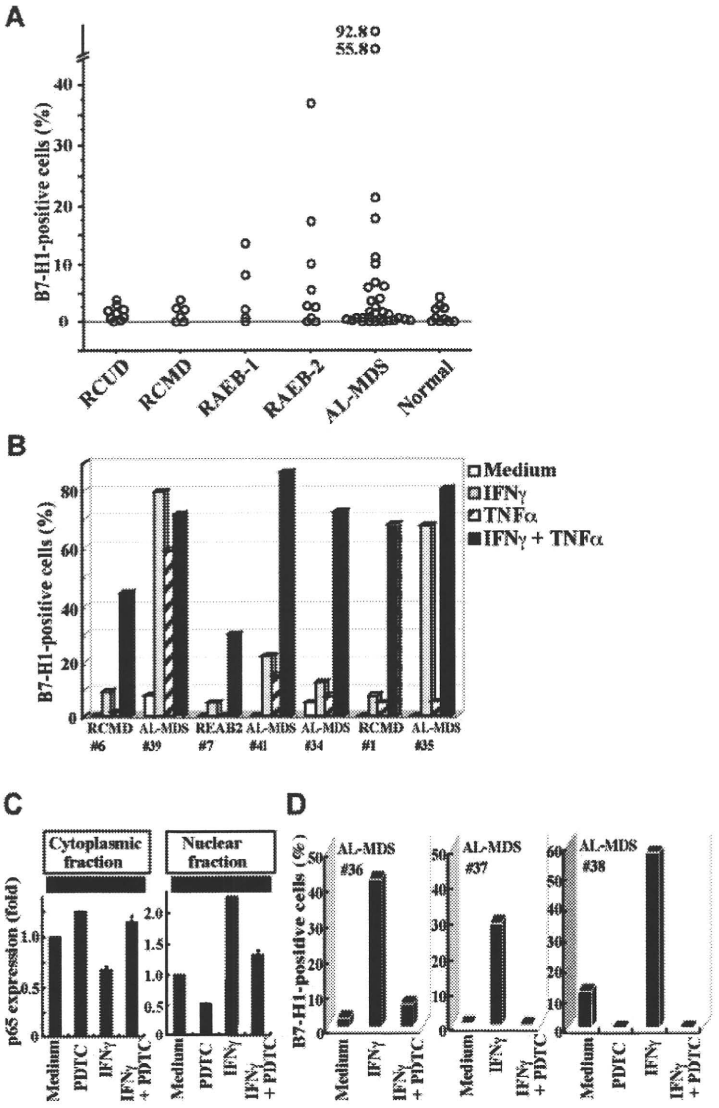

Figure 5. B7-H1 expression on patient blasts. (A) The percentages of B7-H1$^+$ cells in blasts from freshly isolated bone marrow samples. (B) The induction of B7-H1 expression on blasts from 7 patients. The cells had been cultured for 2 days with IFNγ and/or TNFα. (C) Purified CD34$^+$ blasts from a patient (no. 38) were incubated with no additive (Medium), PDTC (100μM), IFNγ, or IFNγ and PDTC. After incubation, the blasts were separated into cytoplasmic and nuclear fractions. The NF-κB p65 contents in each fraction were analyzed using Western blotting to show representative (top panel) and quantified (bottom panel) data (mean + SD) of 2 experiments. In each experiment, the band intensity of cell fractions from blasts that had been cultured with no additive was defined as 1. (E) The inhibitor of NF-κB, PDTC, blocked B7-H1 induction by IFNγ on patient blasts. Purified CD34$^+$ blasts from patients were cultured as indicated, and their B7-H1 expression was analyzed.

Proliferative advantage in B7-H1–expressing MDS cell lines

Based on previous studies,[9,31] we speculated that B7-H1$^+$ MDS blasts might have a proliferative advantage over B7-H1$^-$ MDS blasts. Therefore, we compared the cell cycle between B7-H1$^+$ and B7-H1$^-$ cell fractions in F-36P and SKM-1 cells. The latter cells were cultured with IFNγ for 2 days to induce B7-H1 expression before analysis. In both cell lines, B7-H1$^+$ cells had fewer G_0/G_1 phase cells and more S and G_2/M phase cells compared with B7-H1$^-$ cells. All the results showed statistically significant differences between the positive and negative cells, except for S phase–cell data in F-36P cells (Figure 3A-B). Consistent with these data, the B7-H1$^+$ cell population incorporated more BrdU compared with the B7-H1$^-$ cell population in F-36P and SKM-1 cells (Figure 3C). Next, when purified B7-H1$^+$ and B7-H1$^-$ F-36P cells were subjected to the colony-forming assay using methylcellulose, the former formed more colonies compared with the latter cells (Figure 3D). Furthermore, when the expression of *cyclin* genes was compared between B7-H1$^+$ and B7-H1$^-$ F-36P cells, *cyclin D1*, *D2*, and *D3* mRNA levels were higher in the former cells compared with the latter (supplemental Figure 1).

Morphometric analysis showed that B7-H1$^+$ cells were larger in cell and nuclear sizes and more granular in their cytoplasm compared with B7-H1$^-$ cells in both F-36P and SKM-1 cells (supplemental Table 2).

Effects of B7-H1–expressing MDS cell lines on normal T cells

When normal CD3$^+$ T cells were cultured with or without irradiated F-36P cells, the presence of F-36P cells profoundly increased the percentages of T cells showing apoptosis (Figure 4A). The increase in T-cell apoptosis was accompanied by an increase in T cells with activated caspase-3 (Figure 4B). These findings were observed again when purified CD4$^+$ and CD8$^+$ cells were used instead of the entire CD3$^+$ T-cell population. Furthermore, the apoptosis and caspase-3 activation in T cells induced by F-36P cells were inhibited when the blocking antibody for either B7-H1 or PD-1 was added to the cocultures (analyses of annexin V$^+$PI$^+$ cells showed essentially the same results; Figure 4A-B). Consistent with these findings, the T-cell proliferation in the above allogeneic coculture system was augmented when anti–B7-H1 or anti–PD-1 blocking antibody was added to the culture (Figure 4C). Finally, when purified B7-H1$^+$ or B7-H1$^-$ F-36P cells were used instead of whole F-36P cells, the degree of T-cell apoptosis was higher in the B7-H1$^+$ cell cultures than in the B7-H1$^-$ cell cultures (Figure

4D). These results thus indicate that B7-H1 molecules on F-36P cells increase T-cell apoptosis and decrease T-cell proliferation.

B7-H1 molecules on blasts from MDS patients

We then examined B7-H1 expression on BM blasts from patients with MDS or AL-MDS and from hematologically normal subjects (Figure 5A). B7-H1 molecules were expressed in more than 5% of blasts in a substantial proportion of patients with refractory anemia with excess blasts (RAEB) and AL-MDS, but not in any patients with refractory cytopenia with unilineage dysplasia (RCUD) and refractory cytopenia with multilineage dysplasia (RCMD) or in normal subjects. When patients were divided into 2 groups according to the IPSS category, a higher proportion of blasts expressed B7-H1 molecules in patients in the intermediate-2 or high category than in patients in the low or intermediate-1 category (mean ± SD, 6.5% ± 8.4% [n = 25] vs 1.4% ± 1.3% [n = 15], $P = .0239$). Furthermore, when BM cells from patients were cultured with cytokines, B7-H1 expression on blasts was induced or enhanced by stimulation with IFNγ or TNFα, and most strikingly by their combination (Figure 5B). This B7-H1 induction in MDS blasts from patients was mediated by NF-κB activation, as seen in MDS cell lines. The nuclear translocation of NF-κB p65, indicating NF-κB activation, was induced by IFNγ and was nearly completely blocked by an inhibitor for NF-κB, PDTC (Figure 5C). Furthermore, B7-H1 expression induced by IFNγ on patient blasts was nearly completely blocked by PDTC (Figure 5D).

Next, the cell cycles of B7-H1$^+$ and B7-H1$^-$ blasts were compared in 3 patients. As observed in the MDS cell lines, the percentages of G_0/G_1 phase cells were lower and those of S and G_2/M phase cells were higher in B7-H1$^+$ blasts than in B7-H1$^-$ blasts from all patients examined (Figure 6A). Consistent with these data, B7-H1$^+$ blasts incorporated more BrdU compared with B7-H1$^-$ blasts in all 3 patients examined (11.1% vs 5.7%, 4.6% vs 0.5%, and 11.2% vs 0.9% in 1 RAEB-2 and 2 AL-MDS patients, respectively). It was also observed that Ki-67 expression was higher in B7-H1$^+$ blasts than in B7-H1$^-$ blasts in all 3 patients examined (15.9% vs 11.5%, 83.4% vs 57.5%, and 39.7% vs 33.5% in 1 RCUD, 1 RAEB-2, and 1 AL-MDS patient, respectively). Contrary to the cell lines, cell and nuclear sizes did not differ between B7-H1$^+$ and B7-H1$^-$ blasts, although B7-H1$^+$ blasts were more granular in their cytoplasm (supplemental Table 2). When blasts from 3 patients, in who B7-H1 expression had been induced by IFNγ and TNFα and then irradiated, were cultured with CD3$^+$ T cells from healthy volunteers, T-cell proliferation was significantly augmented by blocking B7-H1 molecules (Figure 6B).

Finally, we investigated the expression of PD-1, a counter-receptor of B7-H1, on circulating T cells in patients with MDS or AL-MDS. PD-1 expression on CD3$^+$, CD4$^+$, and CD8$^+$ T cells was significantly higher in patients than in hematologically normal subjects. Furthermore, PD-1 expression in patients was increased in T cells expressing HLA-DR, a marker of T-cell activation (supplemental Figure 2).

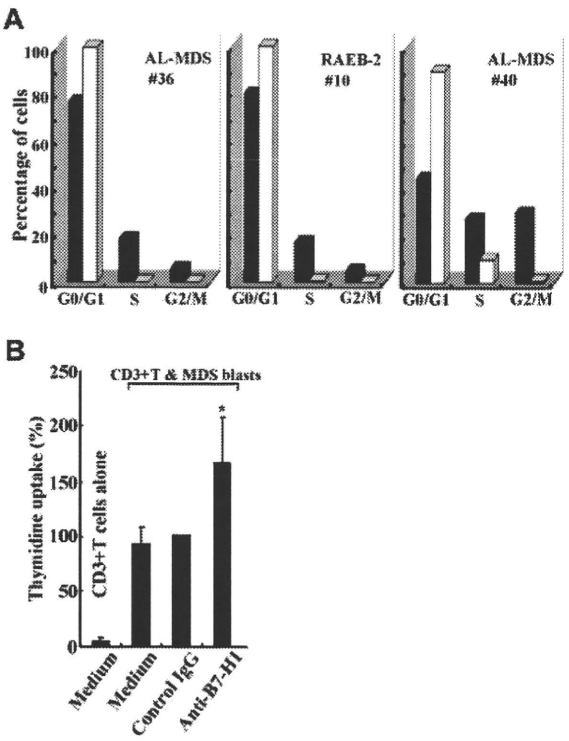

Figure 6. Functional aspects of B7-H1-expressing blasts from patients. (A) Cell cycle of purified CD34$^+$ blasts as a function of B7-H1 expression. Freshly isolated blasts that markedly expressed B7-H1 molecules (from patient no. 36) and blasts cultured with IFNγ and TNFα to induce B7-H1 expression (from patient no. 10 and patient no. 40) were analyzed. B7-H1$^+$ (■) and B7-H1$^-$ (□) cells are indicated. (B) B7-H1–expressing patient blasts were cultured with normal T cells in the presence of control IgG or anti–B7-H1 monoclonal antibodies or medium alone. Data are mean (and SD) of 3 experiments; in each experiment using a different patient sample, data labeled control IgG were defined as 100%. *$P = .026$ compared with control IgG.

Discussion

This study showed that blasts from MDS patients in high-risk IPSS categories express B7-H1 molecules more often compared with blasts from other patients. B7-H1 expression on MDS blasts was induced by IFNγ and TNFα via NF-κB activation, and B7-H1$^+$ MDS blasts had greater proliferative capacity than B7-H1$^-$ MDS blasts. Furthermore, B7-H1$^+$ blasts suppressed T-cell proliferation and induced T-cell apoptosis. Finally, PD-1 expression levels on circulating T cells were higher in MDS patients, in particular in association with the increased HLA-DR expression on T cells, compared with those in healthy volunteers. The morphometric difference observed between B7-H1$^+$ and B7-H1$^-$ MDS blasts may reflect a biologic difference between these 2 cell populations. We believe that B7-H1$^+$ MDS blasts are clonal cells because we confirmed a cytogenetic aberration in B7-H1$^+$ MDS blasts in 2 cases examined (data not shown) and because all patients in whom 5% or more blasts expressed B7-H1$^+$ were in advanced disease stages in which most blasts are clonal.[38]

When T cells are activated, for example, by tumor-associated antigen, they express PD-1 molecules on their surface and produce IFNγ and TNFα.[39] These cytokines suppress colony formation of normal hematopoietic cells and induce apoptosis in hematopoietic cells.[40] In MDS patients, IFNγ and TNFα are often overproduced by PB cells[41] and by macrophages, one of the stromal components, in the BM.[42] These cytokines may also be associated with increased apoptosis of hematopoietic cells. It was also reported that an increased serum TNFα level was associated with leukemic transformation in MDS.[43] Based on these findings and in conjunction with the data in the present study, it is speculated that overproduction of IFNγ and TNFα in the BM microenvironment induces B7-H1 expression on MDS blasts, leading to disease progression at least in some cases by inducing T-cell apoptosis as well as by their intrinsic linkage with a high proliferative potential.

It was reported that constitutive activation of NF-κB in MDS blasts was observed in patients in advanced IPSS categories.[36]

Moreover, this constitutive activation of NF-κB was associated with antiapoptotic features of blasts in those MDS patients.[36] The present results suggest a new mechanism of NF-κB in MDS pathophysiology: by inducing B7-H1 expression on MDS blasts, NF-κB confers a growth advantage on the blasts. The finding that B7-H1$^+$ MDS blasts had greater proliferative capacity than B7-H1$^-$ MDS blasts is interesting. Similarly, Ghebeh et al[44] examined patient breast cancer cells and found that high B7-H1 expression was associated with high Ki-67 expression, a marker of cell proliferation. It has been accepted that B7-H1 acts as a ligand for PD-1 and thus transmits signals to PD-1–expressing cells. However, recent data from one of our groups have shown that the interaction between B7-H1 molecules on murine cancer cells (mastocytoma and renal cell carcinoma) and PD-1 molecules on T cells induces a bidirectional signal: the PD-1–mediated signal inducing T-cell apoptosis and B7-H1–mediated reverse signal inducing cancer cell resistance to apoptosis.[45] Thus, one scenario is that there is a B7-H1–mediated reverse signal to MDS blasts that is associated with their growth advantage.

The inhibitory signal to T cells from the interaction between B7-H1 and PD-1 molecules plays a crucial role in regulating various immune responses. For example, appropriate T-cell regulation by this signal is important to suppress harmful autoimmunity as well as the success of allogeneic transplantation.[46,47] Meanwhile, this inhibitory signal may be used by some types of cancer cell as one strategy to evade the host anticancer immune response. We conclude that this strategy is seen in at least some MDS patients to evade the anti-MDS immune response. We reported that T-cell apoptosis was increased in MDS and that its degree was particularly extensive in advanced disease stages and correlated with the degree of lymphopenia that is common in MDS.[16] We speculate that the signal from B7-H1 molecules on MDS blasts to PD-1 molecules on T cells is one mechanism of the increased T-cell apoptosis observed in MDS patients.

In summary, to the best of our knowledge this is the first report examining the B7-H1 and PD-1 system in MDS in detail. Our results suggest that this system is involved in the pathophysiology in MDS, at least in some patients, by suppressing T-cell immunology and conferring a growth advantage on MDS blasts.

Acknowledgment

This work was supported in part by a Grant-in-Aid for Scientific Research from the Japan Society for the Promotion of Science (20591157).

Authorship

Contribution: A.K. performed experiments and drafted the manuscript; T.Y. and W.Z. performed experiments; H. Tamura conceived and designed the study, supported clinical aspects, and wrote the manuscript; T.T., M.S., E.S., and H. Takahashi supported technical aspects; K.T. and L.C. supported intellectual aspects; K.D. provided administrative and clinical support; and K.O. designed the study, supported clinical aspects, and wrote the manuscript.

Conflict-of-interest disclosure: The authors declare no competing financial interests.

Correspondence: Hideto Tamura, Division of Hematology, Nippon Medical School, 1-1-5 Sendagi, Bunkyo-ku, Tokyo 113-8603, Japan; e-mail: tam@nms.ac.jp.

References

1. Dong H, Zhu G, Tamada K, Chen L. B7-H1, a third member of the B7 family, co-stimulates T-cell proliferation and interleukin-10 secretion. *Nat Med.* 1999;5(12):1365-1369.
2. Tamura H, Dong H, Zhu G, et al. B7-H1 costimulation preferentially enhances CD28-independent T-helper cell function. *Blood.* 2001;97(6):1809-1816.
3. Wang S, Bajorath J, Flies DB, Dong H, Honjo T, Chen L. Molecular modeling and functional mapping of B7-H1 and B7-DC uncouple costimulatory function from PD-1 interaction. *J Exp Med.* 2003; 197(9):1083-1091.
4. Freeman GJ, Long AJ, Iwai Y, et al. Engagement of the PD-1 immunoinhibitory receptor by a novel B7 family member leads to negative regulation of lymphocyte activation. *J Exp Med.* 2000;192(7): 1027-1034.
5. Ishida Y, Agata Y, Shibahara K, Honjo T. Induced expression of PD-1, a novel member of the immunoglobulin gene superfamily, upon programmed cell death. *EMBO J.* 1992;11(11):3887-3895.
6. Dong H, Strome SE, Salomao DR, et al. Tumor-associated B7-H1 promotes T-cell apoptosis: a potential mechanism of immune evasion. *Nat Med.* 2002;8(8):793-800.
7. Yamamoto R, Nishikori M, Tashima M, et al. B7-H1 expression is regulated by MEK/ERK signaling pathway in anaplastic large cell lymphoma and Hodgkin lymphoma. *Cancer Sci.* 2009; 100(12):2093-2100.
8. Thompson RH, Gillett MD, Cheville JC, et al. Costimulatory B7-H1 in renal cell carcinoma patients: indicator of tumor aggressiveness and potential therapeutic target. *Proc Natl Acad Sci U S A.* 2004;101(49):17174-17179.
9. Ghebeh H, Mohammed S, Al-Omair A, et al. The B7-H1 (PD-L1) T lymphocyte-inhibitory molecule is expressed in breast cancer patients with infiltrating ductal carcinoma: correlation with important high-risk prognostic factors. *Neoplasia.* 2006; 8(3):190-198.
10. Konishi J, Yamazaki K, Azuma M, Kinoshita I, Dosaka-Akita H, Nishimura M. B7-H1 expression on non-small cell lung cancer cells and its relationship with tumor-infiltrating lymphocytes and their PD-1 expression. *Clin Cancer Res.* 2004; 10(15):5094-5100.
11. Strome SE, Dong H, Tamura H, et al. B7-H1 blockade augments adoptive T-cell immunotherapy for squamous cell carcinoma. *Cancer Res.* 2003;63(19):6501-6505.
12. Hirano F, Kaneko K, Tamura H, et al. Blockade of B7-H1 and PD-1 by monoclonal antibodies potentiates cancer therapeutic immunity. *Cancer Res.* 2005;65(3):1089-1096.
13. Thompson RH, Kuntz SM, Leibovich BC, et al. Tumor B7-H1 is associated with poor prognosis in renal cell carcinoma patients with long-term follow-up. *Cancer Res.* 2006;66(7):3381-3385.
14. Saudemont A, Quesnel B. In a model of tumor dormancy, long-term persistent leukemic cells have increased B7-H1 and B7.1 expression and resist CTL-mediated lysis. *Blood.* 2004;104(7): 2124-2133.
15. Bynoe AG, Scott CS, Ford P, Roberts BE. Decreased T helper cells in the myelodysplastic syndromes. *Br J Haematol.* 1983;54(1):97-102.
16. Shioi Y, Tamura H, Yokose N, Satoh C, Dan K, Ogata K. Increased apoptosis of circulating T cells in myelodysplastic syndromes. *Leuk Res.* 2007;31(12):1641-1648.
17. Hamblin T. Immunologic abnormalities in myelodysplastic syndromes. *Hematol Oncol Clin North Am.* 1992;6(3):571-586.
18. Parker JE, Mufti GJ, Rasool F, Mijovic A, Devereux S, Pagliuca A. The role of apoptosis, proliferation, and the Bcl-2-related proteins in the myelodysplastic syndromes and acute myeloid leukemia secondary to MDS. *Blood.* 2000;96(12): 3932-3938.
19. Ogata K, Nakamura K, Yokose N, et al. Clinical significance of phenotypic features of blasts in patients with myelodysplastic syndrome. *Blood.* 2002;100(12):3887-3896.
20. Ogata K, Yokose N, Ito T, et al. Assessment of therapeutic potential of interleukin 2 for myelodysplastic syndromes. *Br J Haematol.* 1994;86(3):562-567.
21. Kordasti SY, Ingram W, Hayden J, et al. CD4+CD25high Foxp3+ regulatory T cells in myelodysplastic syndrome (MDS). *Blood.* 2007;110(3): 847-850.
22. Teo SK. Properties of thalidomide and its analogues: implications for anticancer therapy. *AAPS J.* 2005;7(1):E14-E19.
23. List AF. Emerging data on IMiDs in the treatment of myelodysplastic syndromes (MDS). *Semin Oncol.* 2005;32(4 suppl 5):S31-S35.
24. Drexler HG, Dirks WG, Macleod RA. Many are called MDS cell lines: one is chosen. *Leuk Res.* 2009;33(8):1011-1016.
25. Brunning RD, Orazi A, Germing U, et al. Myelodysplastic Syndromes. In: Swerdlow SH, Campo E, Harris NL, et al, eds. *WHO Classification of Tumours of Haematopoietic and Lymphoid Tissues.* Lyon, France: International Agency for Research on Cancer; 2008:87-103.
26. Greenberg P, Cox C, LeBeau MM, et al. International scoring system for evaluating prognosis in myelodysplastic syndromes. *Blood.* 1997;89(6): 2079-2088.

27. Satoh C, Tamura H, Yamashita T, Tsuji T, Dan K, Ogata K. Aggressive characteristics of myeloblasts expressing CD7 in myelodysplastic syndromes. *Leuk Res.* 2009;33(2):326-331.
28. Tamura H, Dan K, Tamada K, et al. Expression of functional B7-H2 and B7.2 costimulatory molecules and their prognostic implications in de novo acute myeloid leukemia. *Clin Cancer Res.* 2005;11(16):5708-5717.
29. Ogata K, Kishikawa Y, Satoh C, Tamura H, Dan K, Hayashi A. Diagnostic application of flow cytometric characteristics of CD34+ cells in low-grade myelodysplastic syndromes. *Blood.* 2006; 108(3):1037-1044.
30. Takada Y, Aggarwal BB. Flavopiridol inhibits NF-kappaB activation induced by various carcinogens and inflammatory agents through inhibition of IkappaBalpha kinase and p65 phosphorylation: abrogation of cyclin D1, cyclooxygenase-2, and matrix metalloprotease-9. *J Biol Chem.* 2004; 279(6):4750-4759.
31. Yamashita T, Tamura H, Satoh C, et al. Functional B7.2 and B7-H2 molecules on myeloma cells are associated with a growth advantage. *Clin Cancer Res.* 2009;15(3):770-777.
32. Cheshire JL, Baldwin AS Jr. Synergistic activation of NF-kappaB by tumor necrosis factor alpha and gamma interferon via enhanced I kappaBalpha degradation and de novo I kappaBbeta degradation. *Mol Cell Biol.* 1997;17(11):6746-6754.
33. Deb A, Haque SJ, Mogensen T, Silverman RH, Williams BR. RNA-dependent protein kinase PKR is required for activation of NF-kappaB by IFN-gamma in a STAT1-independent pathway. *J Immunol.* 2001;166(10):6170-6180.
34. Luo JL, Kamata H, Karin M. IKK/NF-kappaB signaling: balancing life and death–a new approach to cancer therapy. *J Clin Invest.* 2005;115(10): 2625-2632.
35. Chen Y, Zhang J, Guo G, et al. Induced B7-H1 expression on human renal tubular epithelial cells by the sublytic terminal complement complex C5b-9. *Mol Immunol.* 2009;46(3):375-383.
36. Braun T, Carvalho G, Coquelle A, et al. NF-kappaB constitutes a potential therapeutic target in high-risk myelodysplastic syndrome. *Blood.* 2006;107(3):1156-1165.
37. Fabre C, Carvalho G, Tasdemir E, et al. NF-kappaB inhibition sensitizes to starvation-induced cell death in high-risk myelodysplastic syndrome and acute myeloid leukemia. *Oncogene.* 2007; 26(28):4071-4083.
38. Bernell P, Jacobsson B, Nordgren A, Hast R. Clonal cell lineage involvement in myelodysplastic syndromes studied by fluorescence in situ hybridization and morphology. *Leukemia.* 1996;10(4): 662-668.
39. Thompson RH, Dong H, Lohse CM, et al. PD-1 is expressed by tumor-infiltrating immune cells and is associated with poor outcome for patients with renal cell carcinoma. *Clin Cancer Res.* 2007; 13(6):1757-1761.
40. Maciejewski J, Selleri C, Anderson S, Young NS. Fas antigen expression on CD34+ human marrow cells is induced by interferon gamma and tumor necrosis factor alpha and potentiates cytokine-mediated hematopoietic suppression in vitro. *Blood.* 1995;85(11):3183-3190.
41. Koike M, Ishiyama T, Tomoyasu S, Tsuruoka N. Spontaneous cytokine overproduction by peripheral blood mononuclear cells from patients with myelodysplastic syndromes and aplastic anemia. *Leuk Res.* 1995;19(9):639-644.
42. Kitagawa M, Saito I, Kuwata T, et al. Overexpression of tumor necrosis factor (TNF)-alpha and interferon (IFN)-gamma by bone marrow cells from patients with myelodysplastic syndromes. *Leukemia.* 1997;11(12):2049-2054.
43. Symeonidis A, Kourakli A, Katevas P, et al. Immune function parameters at diagnosis in patients with myelodysplastic syndromes: correlation with the FAB classification and prognosis. *Eur J Haematol.* 1991;47(4):277-281.
44. Ghebeh H, Tulbah A, Mohammed S, et al. Expression of B7-H1 in breast cancer patients is strongly associated with high proliferative Ki-67-expressing tumor cells. *Int J Cancer.* 2007;121(4): 751-758.
45. Azuma T, Yao S, Zhu G, Flies AS, Flies SJ, Chen L. B7-H1 is a ubiquitous antiapoptotic receptor on cancer cells. *Blood.* 2008;111(7):3635-3643.
46. Wang L, Han R, Hancock WW. Programmed cell death 1 (PD-1) and its ligand PD-L1 are required for allograft tolerance. *Eur J Immunol.* 2007; 37(10):2983-2990.
47. Fife BT, Bluestone JA. Control of peripheral T-cell tolerance and autoimmunity via the CTLA-4 and PD-1 pathways. *Immunol Rev.* 2008;224:166-182.

Published online 9 September 2010

Nucleic Acids Research, 2011, Vol. 39, No. 2 ***589–598***
doi:10.1093/nar/gkq794

HIV-1 RT-dependent DNAzyme expression inhibits HIV-1 replication without the emergence of escape viruses

Ryuichi Sugiyama[1], Masaaki Hayafune[1], Yuichiro Habu[2,3], Norio Yamamoto[4] and Hiroshi Takaku[1,2,*]

[1]Department of Life and Environmental Science, [2]High Technology Research Center, Chiba Institute of Technology, 2-17-1 Tsudanuma, Narashino-shi, Chiba 275-0016, Japan, [3]Department of Microbiology, Immunology and Pathology 1619 Campus Delivery, Colorado State University, Fort Collins, CO 80523-161, USA and [4]Influenza Virus Research Center, National Institute of Infectious Diseases, 4-7-1 Musashimurayama-shi, Tokyo 208-0011, Japan

Received June 2, 2009; Revised August 18, 2010; Accepted August 23, 2010

ABSTRACT

DNAzymes are easier to prepare and less sensitive to chemical and enzymatic degradation than ribozymes; however, a DNA enzyme expression system has not yet been developed. In this study, we exploited the mechanism of HIV-1 reverse transcription (RT) in a DNA enzyme expression system. We constructed HIV-1 RT-dependent lentiviral DNAzyme expression vectors including the HIV-1 primer binding site, the DNA enzyme, and either a native tRNA (Lys-3), tR^MDtR^L, or one of two truncated tRNAs (Lys-3), $tR^MD\Delta ARMtR^L$ or tR^MD3'-$endtR^L$. Lentiviral vector-mediated DNAzyme expression showed high levels of inhibition of HIV-1 replication in SupT1 cells. We also demonstrated the usefulness of this approach in a long-term assay, in which we found that the DNAzymes prevented escape from inhibition of HIV. These results suggest that HIV-1 RT-dependent lentiviral vector-derived DNAzymes prevent the emergence of escape mutations.

INTRODUCTION

RNAi has emerged as a powerful tool for probing the function of genes of a known sequence both *in vitro* and *in vivo*. Recent studies describe the ability of RNAi to decrease the replication of human immunodeficiency virus type 1 (HIV-1) in lymphocytes using siRNAs targeting viral proteins (for example, *tat*, *gag*, *rev*, *env* and *nef*) (1–9) as well as host proteins (for example, CCR5 and CD4) (10–12). Thus, this technique has the potential to be used as a form of gene therapy for HIV-1 and associated infections. More recently, several groups have reported that the antiviral activity of short hairpin RNA (shRNAs) targeting HIV-1 is abolished owing to the emergence of viral quasi-species harboring a point mutation in the shRNA target region (13–16). This finding is particularly relevant for viruses that exhibit significant genetic variation due to error-prone replication machinery, and the risk is likely to be more severe for RNA viruses and retroviruses than for DNA viruses.

Ribozyme technologies are major tools used to inactivate genes in gene therapy (17–19). One model, termed the deoxyribozyme (Dz) model, is especially useful because it can bind and cleave any single-stranded RNA at purine/pyrimidine junctions (20–22). The DNAzyme is similar to hammerhead ribozymes in terms of its secondary structure, which contains two binding arms and a catalytic loop that captures the indispensable catalytic metal ions (23–25). Previously, we described a new system designed for single-stranded DNA (ssDNA) expression using HIV-1 reverse transcriptase (26). The expressed DNAzymes were shown to possess *in vitro* site-specific cleavage activity.

Here, we describe the inhibition of HIV-1 replication by an HIV-1 reverse transcription (RT)-dependent lentiviral vector-transduced DNAzyme. In addition, we describe the construction of a lentiviral vector encoding the DNAzyme, the HIV-1 primer binding site, a native transfer RNA $(tRNA)^{Lys-3}$, and the flanking arms complementary to the HIV-1 V3-loop of the *env* messenger RNA (mRNA) (10,25–28) downstream of the Pol III promoters, $tRNA_i^{Met}$ (29) or U6 (30). The HIV-1 RT-dependent lentiviral vector-transduced DNAzyme inhibited HIV-1 replication and prevented the emergence of resistant viruses in long-term assays.

*To whom correspondence should be addressed. Tel: +81 47 478 0407; Fax: +81 47 471 8764; Email: hiroshi.takaku@it-chiba.ac.jp

The authors wish it to be known that, in their opinion, the first two authors should be regarded as joint First Authors.

MATERIALS AND METHODS

Construction of lentiviral vectors

Plasmids pVAX-Dz-tRNA^{Lys-3}-ter, pVAX-Dz-ΔARMtRNA^{Lys-3}-ter and pVAX-Dz-3′-endtRNA^{Lys-3}-ter were constructed as described earlier (26) and digested with *Kpn* I and *Eco*R I. DNA was then extracted with phenol/chloroform, precipitated with ethanol, and ligated into the *Kpn* I and *Eco*R I sites of pSV2neo (L6) (31) with the tRNA$_i^{Met}$ promoter (29). DNAzyme expression vectors (pL6-tRNA$_i^{Met}$-Dz-tRNA^{Lys-3}-ter, pL6-tRNA$_i^{Met}$-Dz-ΔARMtRNA^{Lys-3}-ter and pL6-tRNA$_i^{Met}$-Dz-3′-endtRNA^{Lys-3}-ter) were digested with *Eco*R I and then cloned into the same site in the lentiviral transfer vector (CS-CDF-CG-PRE).

The shRNA sequences were chemically synthesized as two complementary DNA oligonucleotides: 5′-GACAAG CACATTCTAACATTTCAAGAGAATGTTAGAATG TGCTTGTCTTTTTGGGCCC-3′ and 5′-TCGAGGGCC CAAAAAGACAAGCACATTCTAACATTCTCTTGA AATGTTAGAATGTGCTTGTCGTAC-3′. These oligonucleotides were annealed and ligated into pU6-ter (*Kpn* I and *Xho* I cloning sites). pU6-shRNA-ter, pU6-Dz-tRNA^{Lys3}-ter, pU6-Dz-3′-endtRNA^{Lys3}-ter and the controls, pU6-ter and pU6-Dz-I-3′-endtRNA^{Lys3}-ter (DNAzyme with an inverted catalytic core sequence) (32,33), were each digested with *Eco*R I and *Nhe* I and then cloned into the same sites in the CS-CDF-CG-PRE vector.

Cell culture

SupT1 and 293T cells were grown in RPMI 1640 medium or Dulbecco's modified Eagle's medium (Sigma-Aldrich Co., St Louis, MO, USA) supplemented with 10% (v/v) heat-inactivated fetal bovine serum, penicillin (100 U/ml) and streptomycin (100 μg/ml). All cultures were maintained at 37°C under a 5% CO_2 atmosphere.

RT–PCR analysis (RNA expression)

Total RNA from vector-transduced cells was extracted using a GenElute mammalian total RNA kit (Sigma-Aldrich). After isolation, RNA samples were treated with DNase I (Takara Shuzo, Kyoto, Japan) according to the manufacturer's specifications. Reverse transcription polymerase chain reaction (RT–PCR) was then performed using an RNA PCR high-plus kit (Toyobo, Osaka, Japan) with the following primers: forward primers, 5′-AGCAGAGTGGCGCAGCGGAAG-3′ for the tRNA$_i^{Met}$ promoter F1, 5′-GTACCCAAGCACTCG TT-3′ for the U6 promoter F4 and 5′-GTACCCAAGCAC TTCCGATC-3′ for the U6-D-I-3′-endtR^L F5; and reverse primers, 5′-CACTCGTTACAAGGCTAGCTACAAC-3′ for the tRNA$_i^{Met}$ promoter R1 and 5′-TGGCGCCGAA CAGGGACTT-3′ for the U6 promoter R3. RT–PCR products were amplified using the following thermal cycling program: 60°C for 30 min, 94°C for 2 min, and then 25 cycles at 94°C for 1 min and 50°C for 90 s, followed by 51°C for 7 min. As an internal control, the mRNA of the human control gene glyceraldehyde-3-phosphate dehydrogenase (G3PDH; Accession No. NM_002046.3) was amplified simultaneously using G3PDH-F (nucleotides 628–647) and G3PDH-R (nucleotides 1060–1079) primers.

Southern hybridization

SupT1 cells stably expressing the DNAzyme were infected with HIV-1$_{NL4-3}$. After 8 h, cytoplasmic extracts were obtained using a nuclear extraction kit (Marligen Bioscience, Ijamsville, MD, USA). Cytoplasmic extracts were then digested with RNase (Promega, Madison, WI, USA) according to the manufacturer's specifications and separated by 18% polyacrylamide-8 M urea sequencing gel electrophoresis. Next, the DNA was transferred to Zeta-Probe nylon membranes (Bio-Rad, Hercules, CA, USA). The filters were prehybridized for 1 h at 42°C in ECL gold hybridization buffer (GE Healthcare, Chalfont St Giles, UK) and then incubated for 16 h in hybridization buffer containing DNAzyme- or DNAzyme inverse-specific probes labeled with 5′-biotin (5′-GTACCCAAGCACTCGTTGTAGCTAGCCTTGT AAC-3′ or 5′-GTACCCAAGCACTTCCGATCGATGT TGCTGTAAC-3′). The blots were immersed in a chemiluminescent nucleic acid detection module kit (Pierce, Rockford, IL, USA) according to the manufacturer's instructions and exposed to Kodak XAR-5 film.

RT–PCR analysis (mRNA cleavage)

Total RNA from vector-transduced cells was extracted using a GenElute mammalian total RNA kit (Sigma-Aldrich). RT–PCR was then performed using an RNA PCR high-plus kit (Toyobo) with *env* upstream (NL4-3 7070–7099), *env* neutral (NL4-3 7241–7271) and *env* downstream (NL4-3 7570–7600) forward primers F2 (5′-ACAGCTGAACACATCTGTAGAAATTAATT G-3′) and F3 (5′-AAACAGATAGCTAGCAAATTAAG AGAACAA-3′) and with the reverse primer R2 (5′-GTTG TTATTACCACCATCTCTTGTTAATAG-3′). RT–PCR products were amplified using the following thermal cycling program: 60°C for 30 min, 94°C for 2 min and then 25 cycles of 94°C for 1 min and 53°C for 90 s, followed by 51°C for 7 min. As an internal control, the mRNA of the human control gene G3PDH was amplified simultaneously with G3PDH-F (nucleotides 628–647) and downstream G3PDH-R (nucleotides 1060–1079) primers.

Lentiviral vector preparation

A vector construct (15 μg) was co-transfected into 293T cells with helper constructs encoding gag/pol (pMDLg/p.RRE; 15 μg), the rev-expressing construct pRSV-rev (5 μg), and the VSV-G-expressing construct pMD.G (5 μg), using the calcium phosphate precipitation method. Supernatants were harvested 48 h posttransfection, filtered through a 0.45-μm filter disc, and concentrated 100-fold by centrifugation at 6000*g* overnight. The resultant viral pellet was resuspended in serum-free and antibiotic-free RPMI medium and stored at −80°C until use. To determine the viral titer, SupT1 cells were transduced with the prepared viral stock, and the number of EGFP-positive cells was determined using

flow cytometric analysis (BD Biosciences, Pharmingen, San Diego, CA, USA) after 72 h of culture.

Flow cytometry

Transduced SupT1 cells were washed twice in phosphate-buffered saline (PBS) and then fixed in PBS containing 1% formaldehyde. Direct fluorescence of EGFP was analyzed using a FACSCalibur system (BD Biosciences). Data acquisition and analysis were performed with CellQuest software (BD Biosciences). Gates for EGFP detection were established using mock-transduced cells as a background.

Fluorescence microscopy

We investigated the efficiency of EGFP expression as an index for SupT1 cells expressing the transgenes. For the intracellular fluorescence studies, SupT1 cells were fixed with 3.7% formaldehyde on alternating days. Fluorescent cells were examined under a fluorescence microscope (Biozero BZ-8000; KEYENCE, Osaka, Japan) at an excitation wavelength of 488 nm using a 10× objective lens. Images were acquired at a resolution of 512 × 512.

HIV-1 challenge and culture assay

After transduction with the lentiviral vectors, EGFP-positive SupT1 cells were sorted using a FACSVantage system (Becton Dickinson, Franklin Lakes, NJ, USA) and infected with HIV-1_{NL4-3} or mutant virus HIV-$1_{NL4-3\text{-}env\text{-}mut\text{-}a}$ at a multiplicity of infection of 0.1. After the harvested culture was centrifuged, the cell-free medium was used for an HIV-1 p24 chemiluminescent enzyme immunoassay (Fujirebio, Tokyo, Japan) (34).

Genotypic sequence analysis of the vif siRNA target region of HIV-1_{NL4-3}

Viral RNA from HIV-1_{NL4-3}-challenged CS-env-shRNA transduced cultures was analyzed for siRNA-mediated mutations in the env-shRNA target region at 43 days postinfection, as described earlier (35,36). Viral RNA was isolated from the cell-free culture supernatant using a QIAamp viral RNA kit (Qiagen, Hilden, Germany) according to the manufacturer's protocol. Viral RNA (5 µl) was used in an RT–PCR reaction containing Powerscript reverse transcriptase (Clontech, Mountain View, CA, USA), 1 µM each of the deoxynucleotide triphosphates, 1 × first-strand buffer (Clontech), 200 ng random hexamers (Promega) and 10 U RNasin (Promega). Reverse transcription was performed at 42°C for 1 h, followed by heat inactivation of the reverse transcriptase at 70°C for 15 min. cDNA (2 µl) was added to a 48-µl PCR mixture containing 1 × Qiagen Taq PCR buffer, 1.5 mM $MgCl_2$, 20 pmol each of the sense primer *env* F (5′-ATG GAA AAC AGA TGG CAG GTG AT-3′) and the antisense primer *env* R (5′-CTA GTG TCC ATT CAT TGT ATG GCT-3′), 1 mM deoxynucleotide triphosphates and 2.5 U Taq polymerase (Qiagen). PCR was performed in a gradient PCR thermal cycler (Astec, Fukuoka, Japan) using the following thermal program: 95°C for 1 min and then 35 cycles at 95°C for 15 s, 58°C for 30 s and 72°C for 30 s, followed by 72°C for 5 min. The PCR product was fractionated, analyzed in a 1% SeaKem gel, and purified using a QIAEX II gel extraction kit (Qiagen). Nucleotide sequencing was performed using dye-labeled terminator chemistry.

Generation of viruses

After 43 days, the harvested supernatant containing the *env* mutation virus, HIV-$1_{NL4-3\text{-}env\text{-}mut\text{-}a}$, was titered, stored at −80°C, and later used as the HIV-$1_{NL4-3\text{-}env\text{-}mut}$ virus.

RESULTS

Construction of lentiviral vectors

The design and *in vitro* strategies used to generate the DNAzyme are shown in Figure 1. First, we show the predicted secondary structure of the HIV-1 RT-dependent DNAzyme expression vector (Figure 1A). As shown in Figure 1A, the native $tRNA^{Lys-3}$ or one of two truncated tRNAs-(ΔARMtRNA^{Lys-3} and 3′-endtRNA^{Lys-3})-PBS complexes served as the primer for HIV-1 RT. Next, we constructed the ssDNA lentiviral expression vectors tR^M-D-tR^L, tR^M-D-ΔARMtR^L, tR^M-D-3′-endtR^L, U6-D-tR^L and U6-D-3′-endtR^L containing the DNAzyme, the HIV-1 primer binding site (PBS), and either a native $tRNA^{Lys-3}$ or one of two truncated tRNAs [tR^M-D-ΔARMtR^L, which lacks the D-stem loop, the anticodon-stem loop and the variable loop or tR^M-D-3′-end$tRNA^{Lys-3}$, which lacks the D-stem-loop, the anticodon-stem loop, the variable loop and the 50-end strand from the full-length tRNA (Lys-3)] that are under the control of the $tRNA_i^{Met}$ or U6 promoter (Figure 1B). We also constructed the control lentiviral vectors tR^M, U6, U6-D-I-tR^L (DNAzyme with the inverted catalytic core sequence) (32,33) and U6-env-shRNA (NL4-3 *env* 7193–7213) (8) for comparison with the DNAzyme. Sequences encoding an active fragment of the DNA enzyme that contained the 10–23 catalytic motif (24,37), the HIV-1 primer binding site and three different tRNA lengths (Lys-3) were inserted between the *Kpn* I and *Eco*R I restriction sites of the RNA transcription vector, pVAX1 (Figure 1B). The DNA enzyme sequence was placed between two oligonucleotide arms that were complementary and able to specifically target the HIV-1 *env* mRNA (7196–7210, according to GenBank accession number AF324493; env-Dz of Figure 1C).

DNA expression in human T cells stably expressing the DNAzyme

SupT1 cells were infected with ssDNA lentiviral expression vectors, and the corresponding template RNAs were expressed from the $tRNA_i^{Met}$ promoter (Figure 2A). Total cellular RNA was isolated from SupT1 cells stably expressing the DNAzyme and analyzed by RT–PCR. The template RNA for the DNAzyme, the HIV-1 primer

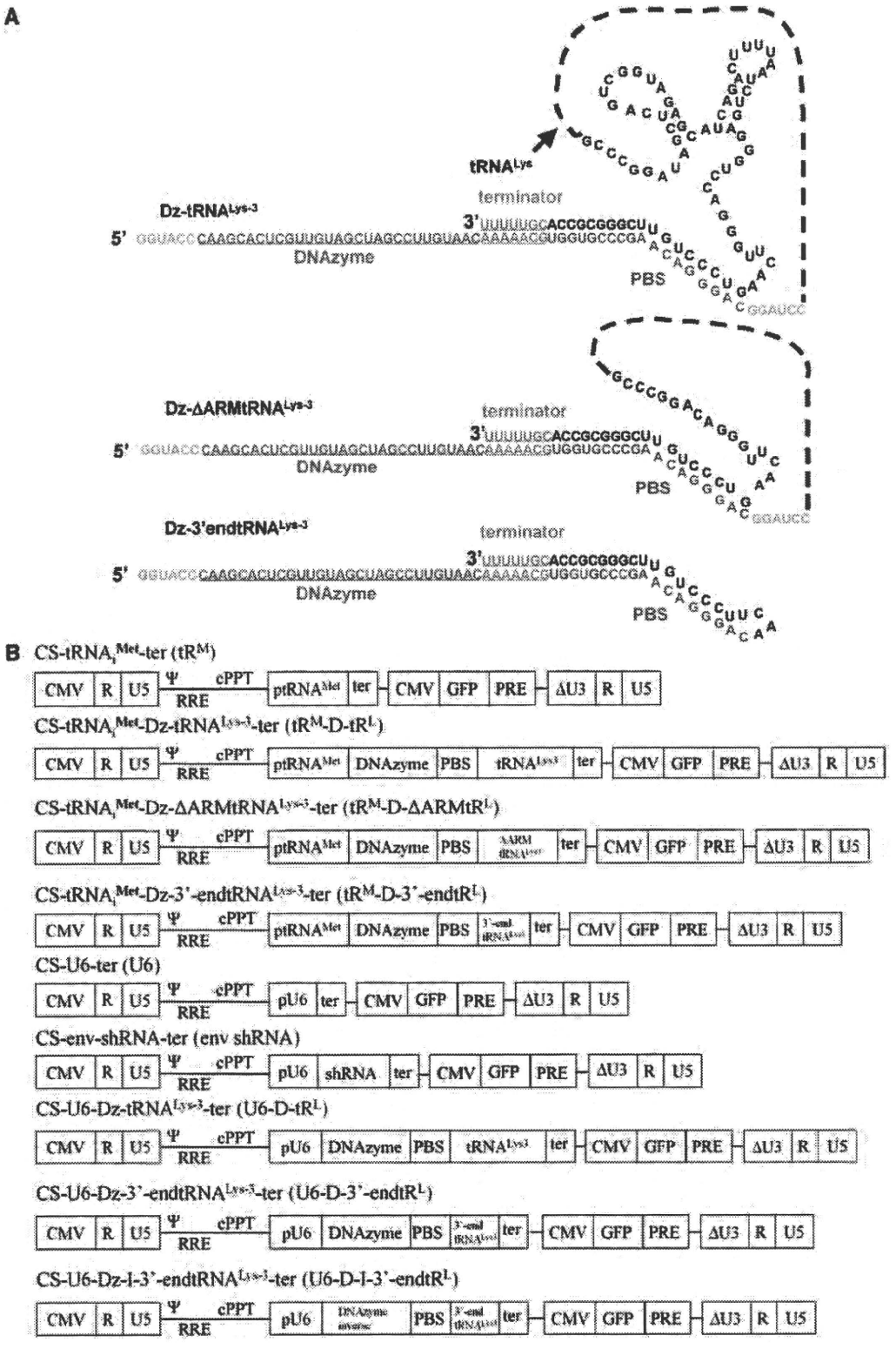

Figure 1. DNAzymes, lentiviral vectors and Dz structures. (**A**) The predicted secondary structure of the ssDNA-expressing lentivirus vector. Sequence of the template RNA containing the DNA enzyme, HIV-1 primer binding site (PBS), and the native $tRNA^{Lys-3}$, $\Delta ARMtRNA^{Lys-3}$ (lacking the D-stem loop, the anticodon-stem loop and the variable loop) and 3′-$endtRNA^{Lys-3}$ (lacking the D-stem loop, the anticodon-stem loop and the variable loop, and the 50 end strand from the full-length $tRNA^{Lys-3}$). (**B**) Lentiviral vector (CS-CDF-CG-PRE) containing the packaging signal (ψ) comprising the 5′-untranslated region (UTR) and 5′-sequences of the Rev-responsive element, the central polypurine tract and the woodchuck hepatitis virus posttranscriptional regulatory element. The 3′-long-terminal repeat contains a large deletion in the U3 region (DU3). CMV, human cytomegalovirus immediate early promoter; EGFP, enhanced green fluorescent protein; $ptRNA^{Met}$, transfer RNA-methionine promoter (tR^{M}); U6, U6 promoter; ter, terminator; D, DNAzyme; PBS, primer binding site; shRNA, short hairpin RNA; D-I, DNAzyme with inverted catalytic core sequence. (**C**) Structure of an active or inactive catalytic (I) motif containing DNAzymes targeting the AU dinucleotides present in the HIV-1 mRNA including the V3-loop of the *env* mRNA region. Cleavage occurs at the position indicated by the arrow.

(continued)

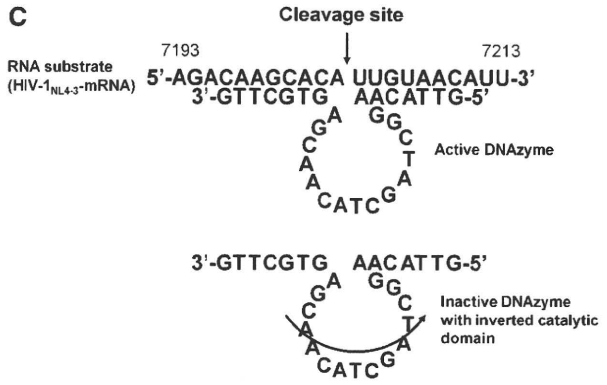

Figure 1. Continued.

binding site and a native $tRNA^{Lys-3}$ driven by the $tRNA_i^{Met}$ promoter were expressed in SupT1 cells stably expressing the DNAzyme (Figure 2A, lanes 2–4). However, the direct expression of RNA from the ssDNA lentiviral expression vector resulted in the expression of sense sequences to HIV-*env* mRNA target regions and consequently did not inhibit HIV-1 replication. The control lentiviral vector, CS-$tRNA_i^{Met}$-ter (tR^M), did not express the corresponding RNA (Figure 2A, lane 1).

Next, to confirm ssDNA expression in SupT1 cells stably expressing the DNAzyme, we infected them with HIV-1_{NL4-3}. Cytoplasmic extracts obtained using digitonin lysis buffer were digested with RNase A, and ssDNA expression was demonstrated by Southern blot

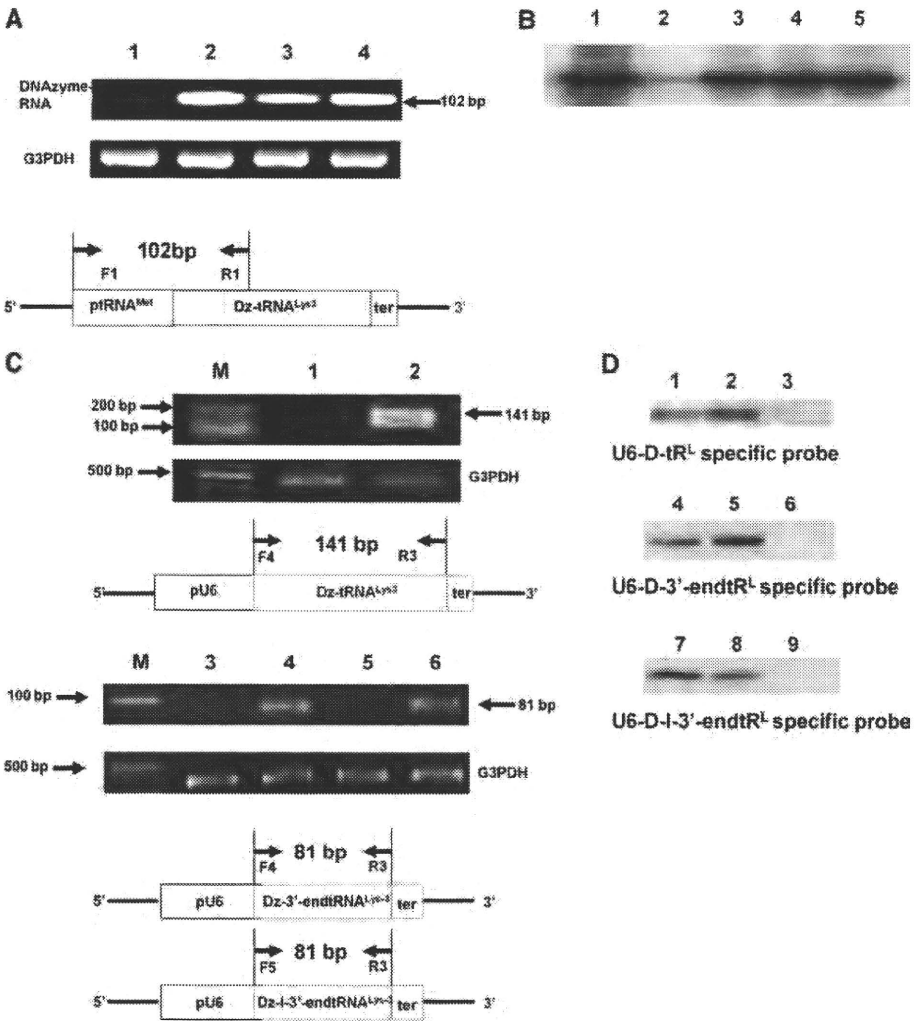

Figure 2. Detection of DNAzyme RNAs and ssDNAs in SupT1 cells stably expressing DNAzyme. (**A**) RT–PCR amplification products of RNAs containing the DNAzyme, HIV-1 PBS and a native $tRNA^{Lys-3}$ driven by the $tRNA_i^{Met}$ promoter. Lane 1, control; lane 2, tR^M-D-tR^L; lane 3, tR^M-D-ΔARMtR^L and lane 4, tR^M-D-3′-endtR^L. (**B**) Detection of ssDNA expression by Southern blot analysis. Lane 1, synthetic ssDNA (102 bp); lane 2, tR^M-D-tR^L-without HIV-1_{NL4-3}; lane 3, tR^M-D-tR^L; lane 4, tR^M-D-ΔARMtR^L and lane 5, tR^M-D-3′-endtR^L. (**C**) RT–PCR amplification of RNAs containing the DNAzyme, HIV-1 PBS and a native $tRNA^{Lys-3}$ driven by the U6 promoter. Lane M, DNA marker; lane 1, U6; lane 2, U6-D-R^L; lane 3, U6; lane 4, U6-D-3′-endtR^L; lane 5, U6; lane 6, U6-D-I-3′-endtR^L. (**D**) Detection of ssDNA expression by Southern blot analysis. Lane 1, synthetic ssDNA (34 bp); lane 2, U6-D-tR^L; lane 3, U6-D-tR^L-without HIV-1_{NL4-3}; lane 4, synthetic ssDNA (34 bp); lane 5, U6-D-3′-endtR^L; lane 6, U6-D-3′-endtR^L without HIV-1_{NL4-3}; lane 7, synthetic ssDNA (34 bp); lane 8, U6-D-I-3′-endtR^L and lane 9, U6-D-I-3′-endtR^L without HIV-1_{NL4-3}.

analysis (Figure 2B). The authentic sample, ssDNA containing the $tRNA_i^{Met}$ promoter, and DNAzyme sequences were synthesized using RT (Figure 2B, lane 1). All ssDNAzymes (tR^M-D-tR^L, tR^M-D-ΔARMtR^L and tR^M-D-3′-endtR^L) were found to be expressed at readily detectable levels (Figure 2B, lanes 3–5). We also examined ssDNA expression in HIV-1-uninfected SupT1 cells stably expressing tR^M-D-tR^L. Although we observed the corresponding template RNA (Figure 2A), the corresponding ssDNAzyme (tR^M-D-tR^L) was not expressed (Figure 2B, lane 2). These data suggest that ssDNA expression is achieved by HIV reverse transcriptase through the template RNA after HIV-1 infection of SupT1 cells stably expressing the DNAzyme.

To compare the U6 and $tRNA_i^{Met}$ promoters, we constructed the ssDNA lentiviral expression vectors U6-D-tR^L and U6-D-3′-endtR^L, which were under the control of the U6 promoter (Figure 1B). The template RNA containing the DNAzymes (U6-D-tR^L and U6-D-3′-endtR^L) was expressed by the lentiviral vectors (U6-D-tR^L and U6-D-3′-endtR^L) in infected SupT1 cells (Figure 2C, lanes 2 and 4). After stable DNAzyme-expressing SupT1 cells (U6-D-tR^L) were challenged with HIV-1_{NL4-3}, cytoplasmic extracts were digested with RNase A, and ssDNA expression was demonstrated by Southern blot analysis. The authentic sample and ssDNA containing the DNAzyme sequences (34 bases) were synthesized by RT (Figure 2D, lanes 1 and 4), and ssDNAzymes (Dz) were found to be expressed at readily detectable levels (Figure 2D, lanes 2 and 5). We also examined ssDNA expression in HIV-1-uninfected SupT1 cells stably expressing U6-D-tR^L and U6-D-3′-endtR^L. The corresponding template RNAs (Figure 2C, lanes 2 and 4), but not the corresponding ssDNAzymes (Figure 2D, lanes 3 and 6), were expressed. Furthermore, the control lentiviral vector U6-D-I-3′-endtR^L (DNAzyme with the inverted catalytic core sequences) also expressed the corresponding template RNA (Figure 2C, lane 6) and ssDNAzyme (Figure 2D, lane 8). ssDNA from the corresponding U6-D-tR^L, U6-D-3′-endtR^L and U6-D-I-3′-endtR^L produced the expected 34-bp band (Figure 2D, lanes 2, 5 and 8).

Long-term inhibition of HIV-1 gene expression by HIV-1 RT-dependent lentiviral vector-derived DNAzyme

To investigate the long-term inhibition of HIV-1 replication, SupT1 cells were stably transduced with the lentiviral expression vectors and then challenged with HIV-1_{NL4-3}. HIV-1 gag p24 antigen levels were measured as an index of viral replication or inhibition by the expressed transgenes at 3 days intervals over a 60 days period. HIV-1 replication was inhibited in SupT1 cells stably expressing the DNAzyme without any viral breakthrough at 60 days postinfection (Figure 3A). By contrast, the control lentiviral vector, tR^M, failed to inhibit viral replication under these experimental conditions. Furthermore, we observed enhanced green fluorescent protein (EGFP) expression at 60 days postinfection in transduced SupT1 cells (Figure 3B). These results suggest that ssDNAzyme expression might initiate from the primer binding site. In SupT1 cells stably expressing env-shRNA, the siRNA-related escape mutant phenomenon was observed at 33 days postinfection in transduced SupT1 cells, as indicated by the virus breakthrough effect (Figure 3A).

To compare the U6 and $tRNA_i^{Met}$ promoters, we examined the long-term inhibition of HIV-1 replication in the different types of stable DNAzyme-expressing SupT1 cells (U6-D-tR^L, U6-D-3′-endtR^L or tR^M-D-tR^L). HIV-1 replication was completely inhibited in all cell types without any viral breakthrough at 60 days postinfection (Figure 3A). By contrast, the controls, U6 and DNAzyme with an inverted catalytic core sequence (U6-D-I-3′-endtR^L) (32,33), showed no inhibitory effect on HIV-1 replication (Figure 3A). We also observed EGFP expression at 60 days postinfection in transduced U6-D-tR^L, U6-D-3′-endtR^L and U6-D-I-3′-endtR^L SupT1 cells (Figure 3B). Therefore, the efficacy of HIV-1 replication inhibition did not differ between these two promoters. Furthermore, our data demonstrated a DNAzyme-specific inhibitory effect on HIV-1 replication, but not an antisense effect.

The inhibitory effect of the DNAzyme occurs via target RNA degradation

The contribution of HIV-1 mRNA degradation to the DNAzyme-mediated anti-HIV-1 effect was examined by measuring HIV-1 mRNA levels. Two sets of RT–PCR reactions were used to establish the level of HIV-1 mRNA at the target site that was not cleaved by DNAzyme (product 1; 529 bp) and the total amount of HIV-1 mRNA cleaved at the target site (product 2; 351 bp). The uncleaved HIV-1 mRNA was amplified using primers F2 and R2 (Figure 4A) (35). The levels of product 1 were expected to decrease after cleavage of the HIV-1 mRNA, whereas the levels of product 2 reflected the total amount of HIV-1 mRNA, as the 3′-fragment of the cleaved HIV-1 mRNA remained a viable template for RT–PCR amplification. We observed that progeny virus production was decreased in cells expressing DNAzyme or shRNA, whereas the control lentiviral vector, tR^{Met}, did not greatly alter uncleaved HIV-1 mRNA expression after 10 days postinfection (Figure 4A). However, after 43 days postinfection, a band of uncleaved HIV-1 mRNA appeared in the shRNA-dependent expression system (Figure 4A, lane 6) but not in the DNAzyme system (Figure 4A, lane 7). Furthermore, the contribution of HIV-1 mRNA cleavage to the DNAzyme-mediated anti-HIV-1 effect was examined by measuring HIV-1 mRNA levels, which revealed that the DNAzyme degraded the target RNA (Figure 4B, lane 3). These data are consistent with the results of the gag-p24 antigen assays and suggest that the inhibitory effect of the DNAzyme is achieved via degradation of the target RNA by the DNAzyme.

Generation of HIV-1 mutants that escape shRNA-env

RNAi has not been shown to protect cells against HIV-1 in long-term virus replication assays. Here the siRNA-related escape mutant phenomenon was observed at 33 days postinfection in transduced SupT1 cells, as

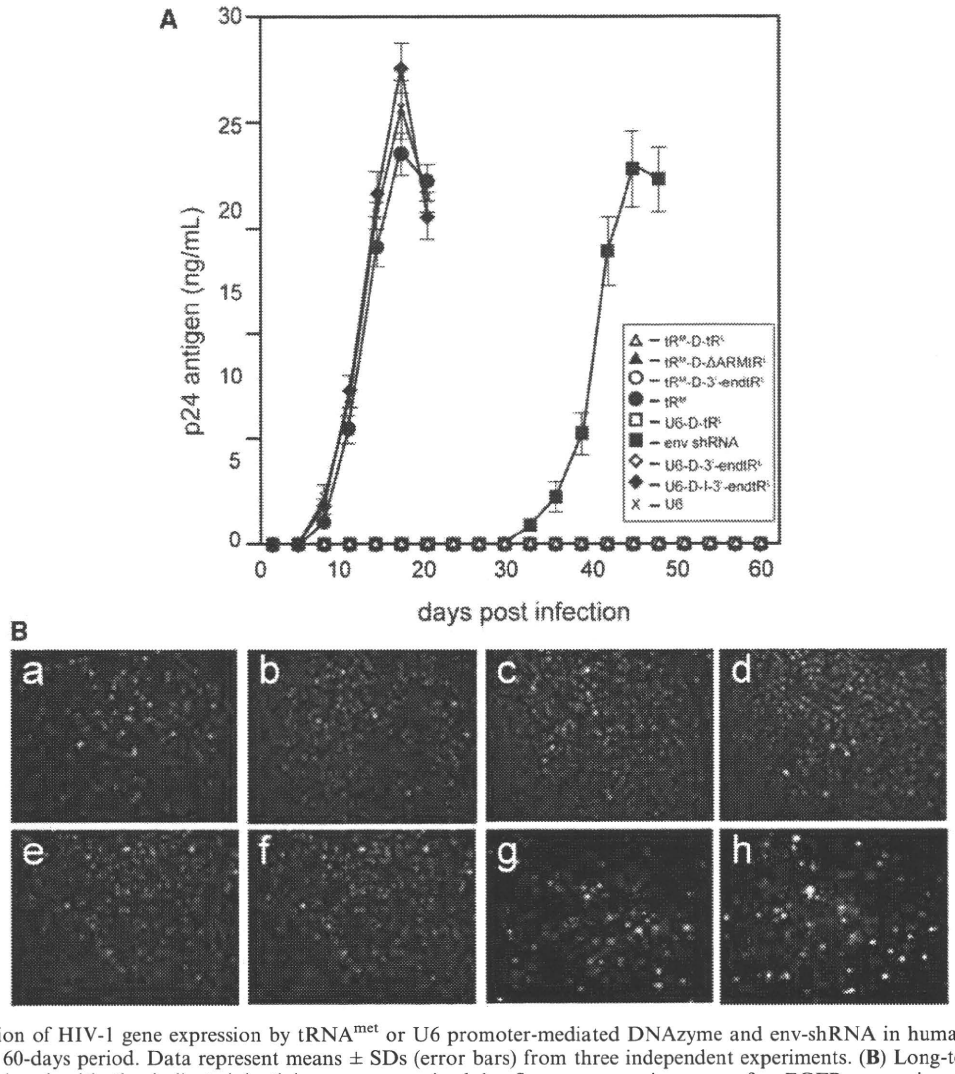

Figure 3. (**A**) Inhibition of HIV-1 gene expression by $tRNA^{met}$ or U6 promoter-mediated DNAzyme and env-shRNA in human T cells. p24 antigen levels assessed over a 60-days period. Data represent means ± SDs (error bars) from three independent experiments. (**B**) Long-term EGFP expression in SupT1 cells transduced with the indicated lentiviruses as examined by fluorescence microscopy for EGFP expression at 60 days following transduction. (a) tR^{M}; (b) tR^{M}-D-tR^{L}; (c) tR^{M}-D-ΔARMtR^{L}; (d) tR^{M}-D-3′-endtR^{L}; (e) U6; (f) U6-D-tR^{L}; (g) U6-D-3′-endtR^{L} and (h) U6-D-I-3′-endtR^{L}.

indicated by the virus breakthrough effect (Figure 3). Therefore, we investigated the sudden surge of viral replication in cultures expressing *env* shRNA; sequence analyses were performed using different cultures (samples mut-a and -b) at 43 days postinfection. This analysis revealed that the RNAi-resistant viruses contained nucleotide substitutions within the shRNA-*env* target sequence (Figure 5A), whereas the DNAzyme sequences remained unchanged (data not shown). These results suggest that the DNAzyme inhibited HIV-1 replication and prevented the emergence of resistant viruses.

To determine whether inhibition of HIV-1 replication was dependent on the DNAzyme, we infected SupT1 cells stably expressing tR^{M}-D-tR^{L} and U6-D-tR^{L} with the evolved HIV-$1_{NL4\text{-}3\text{-}env\text{-}mut\text{-}a}$ carrying mutations corresponding to positions 7201, 7203 and 7206 of the *env* target sequence. Although viral challenge of the DNAzyme-expressing SupT1 cells with HIV-$1_{NL4\text{-}3\text{-}env\text{-}mut\text{-}a}$ did not suppress viral replication (Figure 5B), 92% inhibition was observed in DNAzyme-expressing SupT1 cells with HIV-$1_{NL4\text{-}3}$ over a 60 days period (Figure 3A). This lack of suppressive effects on the HIV-$1_{NL4\text{-}3\text{-}env\text{-}mut\text{-}a}$ strain might be explained by a single base substitution (AU to CU) at the DNAzyme cleavage site. This finding confirms a DNAzyme-mediated anti-HIV-1 effect and not an antisense effect.

DISCUSSION

Recent reports have documented the emergence of virus escape variants following siRNA treatment in long-term cultures (13–17,37) and have raised doubts about the application of siRNA to HIV-1 gene therapy. RNAi-resistant variants can emerge through mutations in siRNA target regions and also through mutations that alter the local RNA structure (38). Furthermore, Bull *et al.* (39) also reported that antisense RNA directed against the viral gene confers resistance to viral replication. However, multiple shRNA gene therapy

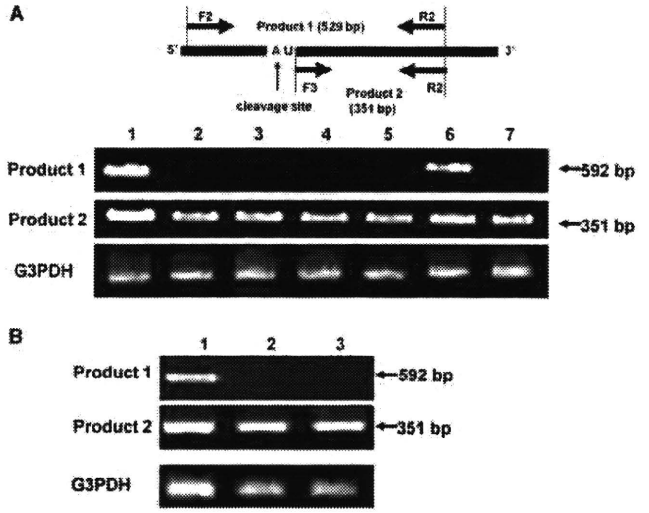

Figure 4. HIV-1 mRNA expression at the target site after treatment with the DNAzyme. (**A**) RT–PCR analyses of uncleaved (product 1) and total cleaved and uncleaved (product 2) HIV-1 mRNA at 10 days posttransfection in SupT1 cells. Lane 1, tR^M; lane 2, tR^M-D-tR^L; lane 3, tR^M-D-ΔARMtR^L; lane 4, tR^M-D-3′-endtR^L; lane 5, env-shRNA; lane 6, env-shRNA, 43 days and lane 7, tR^M-D-tR^L, 43 days. Schematic representation of HIV-1-specific primer sites with respect to HIV-1 mRNA: forward primers F2 and F3 as well as reverse primer R2. (**B**) RT–PCR analyses of uncleaved (product 1) and total cleaved and uncleaved (product 2) HIV-1 mRNA performed using HIV-1 *env*-specific primers with concurrent amplification of G3PDH mRNA. Lane 1, tR^M; lane 2, tR^M-D-tR^L and lane 3, U6-D-tR^L. Schematic representation of HIV-1-specific primer sites with respect to HIV-1 mRNA: forward primers F3 and F4 as well as reverse primer R3.

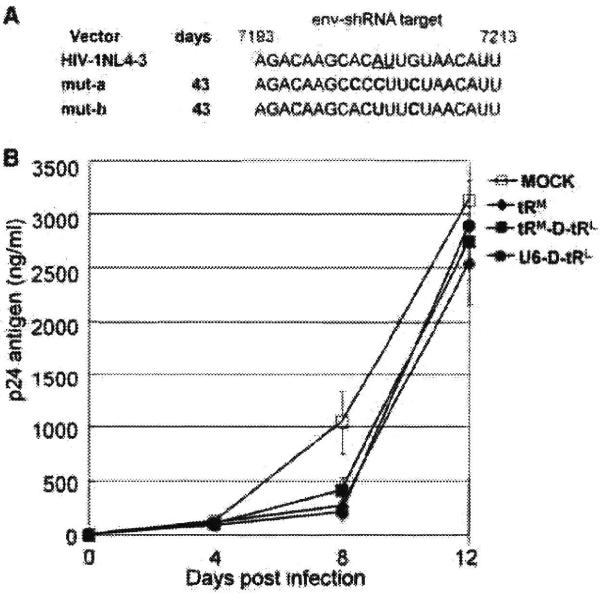

Figure 5. Generation of HIV-1 variants resistant to RNAi. (**A**) Genotype sequence analysis of escape variants. The postinfection day is indicated. The target nucleotides (AU) are underlined. Substitutions are indicated in bold. (**B**) HIV-1 gag-p24 antigen expression in SupT1 cells stably expressing DNAzymes (tR^M-D-tR^L and U6-D-tR^L) that evolved HIV-$1_{NL4\text{-}3\text{-}env\text{-}mut\text{-}a}$ over a 12-days period. Mock: HIV-$1_{NL4\text{-}3\text{-}env\text{-}mut\text{-}a}$. Data represent means ± SDs (error bars) from three independent experiments.

strategies are currently being investigated for the treatment of viral diseases such as HIV-1. It is important to use several different shRNAs to prevent the emergence of treatment-resistant strains (40–43).

Here we propose the use of a DNA rather than an RNA molecule, because the DNAzyme has a secondary structure similar to that of hammerhead ribozymes (23,24,44). Previous studies have shown that the DNAzyme can be expressed by an ssDNA expression vector using HIV-1 reverse transcriptase (28). The ssDNA expression vectors used in the present study contained the DNAzyme, the HIV-1 primer binding site and a native $tRNA^{Lys\text{-}3}$, as well as flanking arms complementary to the HIV-1 V3-loop of the *env* mRNA. However, their anti-HIV-1 activity was low as a result of low posttransfection efficacy of the plasmid DNA vector in human T cells. Recently, Jakobsen *et al.* (45) also reported the efficient inhibition of HIV-1 expression by DNAzymes.

The DNAzyme-induced inhibition of HIV-1 expression was examined in human T cells by constructing an HIV-1 RT-dependent lentiviral ssDNA vector. Lentiviruses integrate into the chromosomal DNA, and therefore their genomes are stable in host cells and are inherited by host cell progeny (46,47). Accordingly, the long-term expression of a transduced gene can be achieved through lentivirus-mediated gene transfer. Other advantages of this vector include its broad host range and the availability of packaging cell lines for the large-scale production of high-titer vectors. The DNAzyme construct was designed to target HIV-1 (NL4-3 *env* 7196–7210), which is more accessible to DNAzyme oligonucleotides. The expression of template RNA containing the DNAzymes driven by the $tRNA_i^{Met}$ or U6 promoters was observed in stable DNAzyme-expressing SupT1 cells [Figure 2A (lanes 2–4) and C (lanes 2, 4 and 6)]. Furthermore, ssDNA expression was achieved from the template RNA by HIV reverse transcriptase [Figure 2B (lanes 3–5) and D (lanes 2, 5 and 8)].

We evaluated the effectiveness of long-term inhibition of HIV-1 replication in HIV-1 RT-dependent lentiviral-mediated DNAzyme-expressing SupT1 cells and found that SupT1 cells stably expressing the DNAzyme showed inhibition of HIV-1 replication for 60 days postinfection (Figure 3A). By contrast, the control lentiviral vectors, tR^M, U6 and U6-D-I-3′-endtR^L (DNAzyme with inverted catalytic core sequence) (32,33), failed to inhibit viral replication under these experimental conditions. These results indicate that DNAzyme-mediated inhibition of HIV-1 replication occurred without an antisense effect. We also found that the primer binding site is required for the expression of ssDNA.

Next, we showed that the effectiveness of the long-term inhibition of HIV-1 replication did not differ under the control of two different promoters: U6 and $tRNA_i^{Met}$ (Figure 3A). The DNAzyme was found to inhibit HIV-1 replication through target RNA degradation (Figure 4A and B), thus preventing the emergence of resistant viruses

(Figure 3A). However, the siRNA-related escape mutant phenomenon was observed in SupT1 cells stably expressing the env-shRNA at 33 days postinfection (Figure 3A). Sequence analyses at 43 days postinfection revealed that the RNAi-resistant viruses contained nucleotide substitutions in the shRNA-*env* target sequence (Figure 5A) (13–17). Furthermore, viral challenge of DNAzyme-expressing (tR^M-D-tR^L and U6-D-tR^L) SupT1 cells with HIV-$1_{NL4\text{-}3\text{-}env\text{-}mut\text{-}a}$ did not suppress viral replication (Figure 5B), demonstrating that DNAzyme-mediated specific silencing of HIV genes significantly inhibited HIV-1 replication. The loss of the inhibitory effect in the HIV-$1_{NL4\text{-}3\text{-}env\text{-}mut\text{-}a}$ strain occurred via a single base mutation (AU to CU) at the DNAzyme cleavage site. Taken together, our results demonstrate the potential of an anti-HIV-1 DNAzyme for controlling HIV-1 infection (22) and preventing the emergence of resistant viruses in long-term assays. More experiments are needed to verify the role of DNAzyme in the inhibition of HIV-1 replication. The results obtained in the present study for DNAzymes might be useful in the development of an effective gene therapy for HIV-1 infections.

ACKNOWLEDGEMENTS

We are grateful to Miss Y. Moori and Y. Mori for their excellent technical assistance. We wish to thank Drs N. Kurosaki and W.S. Park for their participation in helpful discussions.

FUNDING

The Ministry of Health, Labor and Welfare, Japan, Grant-in-Aid for AIDS research; The Ministry of Education, Science, Sports and Culture, Japan, Grant-in-Aid for High Technology Research (HTR); Research Grants from the Human Science Foundation (HIV-K-14719). Funding for open access charge: Ministry of Health, Labor and Welfare, Japan.

Conflict of interest statement. None declared.

REFERENCES

1. Castanotto,D. and Rossi,J.J. (2009) The promises and pitfalls of RNA-interference- based therapeutics. *Nature*, **457**, 426–433.
2. Coburn,G.A. and Cullen,B.R. (2002) Potent and specific inhibition of human immunodeficiency virus type 1 replication by RNA interference. *J. Virol.*, **276**, 9225–9231.
3. Jacque,J., Trioques,K. and Stevenson,M. (2002) Modulation of HIV-1 replication by RNA interference. *Nature*, **418**, 379–380.
4. Lee,N.S., Dohjima,T., Bauer,G., Li,H., Li,M.J., Ehsani,A., Salvaterra,P. and Rossi,J.J. (2002) Expression of small interfering RNAs targeted against HIV-1 rev transcripts in human cells. *Nat. Biotech.*, **20**, 500–505.
5. Novina,C.D., Murray,M.F., Dykxhoorn,D.M., Beresford,P.J., Riess,J.J., Lee,S.K., Collman,R.G., Lieberman,J., Shankar,P. and Sharp,P.A. (2002) siRNA-directed inhibition of HIV-1 infection. *Nat. Med.*, **8**, 681–686.
6. Yamamoto,T., Omoto,S., Mizuguchi,M., Mizukami,H., Okuyama,H., Okada,N., Saksena,N.K., Brisibe,E.A., Otake,K. and Fuji,Y.R. (2002) Double-stranded nef RNA interferes with human immunodeficiency virus type 1 replication. *Microbiol. Immunol.*, **46**, 809–817.
7. Song,E., Lee,S.K., Dykxhoorn,D.M., Novina,C., Zhang,D., Crawford,K., Cerny,J., Sharp,P.A., Lieberman,J., Manjunath,N. *et al.* (2003) Sustained small interfering RNA-mediated human immunodeficiency virus type 1 inhibition in primary macrophages. *J. Virol.*, **77**, 7174–7181.
8. Park,W.S., Hayafune,M., Miyano-Kurosaki,N. and Takaku,H. (2003) Specific HIV-1 env gene silencing by small interfering RNAs in human peripheral blood mononuclear cells. *Gene Ther.*, **10**, 2046–2050.
9. Senserrich,J., Pauls,E., Armand-Ugón,M., Clotet-Codina,I., Moncunill,G., Clotet,B. and Esté,J.A. (2009) HIV-1 resistance to the anti-HIV activity of a shRNA targeting a dual-coding region. *Virology*, **372**, 421–429.
10. Martinez,M.A., Gutierrez,A., Armand-Ugon,M., Blanco,J., Parera,M., Gomez,J., Clotet,B. and Esté,J.A. (2002) Suppression of chemokine receptor expression by RNA interference allows for inhibition of HIV-1 replication. *AIDS*, **16**, 2385–2390.
11. Qin,X.F., An,D.S., Chen,I.S. and Baltimore,D. (2002) Inhibiting HIV-1 infection in human T cells by lentiviral-mediated delivery of small interfering RNA against CCR5. *Proc. Natl Acad. Sci. USA*, **100**, 183–188.
12. Anderson,J., Banerjea,A. and Akkina,R. (2003) Suppression of HIV-1 infection by a stem-loop structured anti-CXCR4 siRNA. *AIDS Res. Hum. Retrovir.*, **19**, 699–706.
13. Boden,D., Pusch,O., Lee,F., Tucker,L. and Ramratnam,B. (2003) Human immunodeficiency virus type 1 escape from RNA interference. *J. Virol.*, **77**, 11531–11535.
14. Das,A.T., Brummelkamp,T.R., Westerhout,E.M., Vink,M., Madiredjo,M., Bernards,R. and Berkhout,B. (2004) Human immunodeficiency virus type 1 escapes from RNA interference-mediated inhibition. *J. Virol.*, **78**, 26001–26005.
15. Nishitsuji,H., Kohara,M., Kannagi,M. and Masuda,T. (2006) Effective suppression of human immunodeficiency virus type 1 through a combination of short- or long-hairpin RNAs targeting essential sequences for retroviral integration. *J. Virol.*, **80**, 7658–7666.
16. Sabariegos,R., Giménez-Barcons,M., Tàpia,N., Clotet,B. and Martínez,M.A. (2006) Sequence homology required by human immunodeficiency virus type 1 to escape from short interfering RNAs. *J. Virol.*, **80**, 571–577.
17. Berkhout,B. (2009) A new Houdini act: multiple routes for HIV-1 escape from RNAi-mediated inhibition. *Future Microbiol.*, **4**, 151–154.
18. Schubert,S. and Kurreck,J. (2004) Ribozyme- and deoxyribozyme-strategies for medical applications. *Curr. Drug Targets*, **8**, 667–681.
19. Joyce,G.F. (2004) Directed evolution of nucleic acid enzymes. *Annu. Rev. Biochem.*, **73**, 791–836.
20. Fiammengo,R. and Jaschke,A. (2005) Nucleic acid enzymes. *Curr. Opin. Biotechnol.*, **6**, 614–621.
21. Sioud,M. and Iversen,P.O. (2005) Ribozymes, DNAzymes and small interfering RNAs as therapeutics. *Curr. Drug Targets*, **6**, 647–653.
22. Santoro,S.W. and Joyce,G.F. (1997) A general purpose RNA-cleaving DNA enzyme. *Proc. Natl Acad. Sci. USA*, **94**, 4262–4266.
23. Santoro,S.W. and Joyce,G.F. (1998) Mechanism and utility of an RNA-cleaving DNA enzyme. *Biochemistry*, **37**, 13330–13342.
24. Breaker,R.R. and Joyce,G.F. (1995) A DNA enzyme with Mg^{2+}-dependent RNA phosphoesterase activity. *Chem. Biol.*, **2**, 655–660.
25. Geyer,C.R. and Sen,D. (1997) Evidence for the metal-cofactor independence of an RNA phosphodiester-cleaving DNA enzyme. *Chem. Biol.*, **4**, 579–593.
26. Kusunoki,A., Miyano-Kurosaki,N. and Takaku,H. (2003) A novel single-stranded DNA enzyme expression system using HIV-1 reverse transcriptase. *Biochem. Biophys. Res. Commun.*, **301**, 535–539.
27. Hayafune,M., Miyano-Kurosaki,N., Kusunoki,A., Mouri,Y. and Takaku,H. (2006) HIV gene therapy using RNA virus systems. *Nucleic Acids Symp. Ser.*, **50**, 79–80.
28. Zhang,X., Xu,Y., Ling,H. and Hattori,T. (1999) Inhibition of infection of incoming HIV-1 virus by RNA-cleaving DNA enzyme. *FEBS Lett.*, **458**, 151–156.

29. Keith,G., Heitzler,J., el Adlouni,C., Glasser,A.L., Fix,C., Desgres,J. and Dirheimer,G. (1993) The primary structure of cytoplasmic initiator tRNA(Met) from *Schizosaccharomyces pombe*. *Nucleic Acids Res.*, **21**, 2949.
30. Medina,M.F. and Hoshi,S. (1999) RNA-polymerase III-driven expression cassettes in human gene therapy. *Curr. Opin. Mol. Ther.*, **1**, 580–594.
31. Habu,Y., Miyano-Kurosaki,N., Kitano,M., Endo,Y., Yukita,M., Ohira,S., Takaku,H., Nashimoto,M. and Takaku,H. (2005) Inhibition of HIV-1 gene expression by retroviral vector-mediated small-guide RNAs that direct specific RNA cleavage by tRNase ZL. *Nucleic Acids Res.*, **33**, 235–243.
32. Khachigian,L.M., Fahmy,R.G., Zhang,G., Bobryshev,Y.V. and Kaniaros,A. (2002) c-Jun regulates vascular smooth muscle cell growth and neointima formation after arterial injury. Inhibition by a novel DNA enzyme targeting c-Jun. *J. Biol. Chem.*, **277**, 22985–92291.
33. Takahashi,H., Hamazaki,H., Habu,Y., Hayashi,M., Abe,T., Miyano-Kurosaki,N. and Takaku,H. (2004) A new modified DNA enzyme that targets influenza virus A mRNA inhibits viral infection in cultured cells. *FEBS Lett.*, **560**, 69–74.
34. Sakai,A., Hirabayashi,Y., Aizawa,S., Tanaka,M., Ida,S. and Oka,S. (1999) Investigation of a new p24 antigen detection system by the chemiluminescence-enzyme-immuno-assay. *J. Japn. Assoc. Infect. Dis.*, **73**, 205–212.
35. Barnor,J.S., Habu,Y., Yamamoto,N., Miyano-Kurosaki,N., Ishikawa,K., Yamamoto,N. and Takaku,H. (2009) Inhibition of HIV-1 replication by long-term treatment with a chimeric RNA containing shRNA and TAR decoy RNA. *Antiviral Res.*, **283**, 156–164.
36. Rosel,K.F. and George,S. (2003) The activity of siRNA in mammalian cells is related to structural target accessibility; a comparison with antisense oligonucleotides. *Nucleic Acids Res.*, **31**, 4417–4425.
37. von Eije,K.J., ter Brake,O. and Berkhout,B. (2008) Human immunodeficiency virus type 1 escape is restricted when conserved genome sequences are targeted by RNA interference. *J. Virol.*, **82**, 2895–2903.
38. Westerhout,E.M., Ooms,M., Vink,M., Das,A.T. and Berkhout,B. (2005) HIV-1 can escape from RNA interference by evolving an alternative structure in its RNA genome. *Nucleic Acids Res.*, **33**, 796–804.
39. Bull,J.J., Jacobson,A., Badgett,M.R. and Molineux,I.J. (1998) Viral escape from antisense RNA. *Mol. Microbiol.*, **28**, 835–846.
40. Li,M.J., Kim,J.D., Li,S.L., Zaia,J.A., Yee,J.K., Anderson,J., Akkina,R. and Rossi,J.J. (2005) Long-term inhibition of HIV-1 infection in primary hematopoietic cells by lentiviral vector delivery of a triple combination of anti-HIV shRNA, anti-CCR5 ribozyme, and a nucleolar-localizing TAR Decoy. *Mol Ther.*, **12**, 900–909.
41. ter Brake,O., Konstantinova,P., Ceylan,M. and Berkhout,B. (2006) Silencing of HIV-1 with RNA interference: a multiple shRNA approach. *Mol. Ther.*, **14**, 883–892.
42. Liu,Y.P., von Eije,K.J., Schopman,N.C., Westerink,J.T., ter Brake,O., Haasnoot,J. and Berkhout,B. (2009) Combinatorial RNAi against HIV-1 using extended short hairpin RNAs. *Mol. Ther.*, **17**, 1712–1723.
43. Anderson,J.S., Javien,J., Nolta,J.A. and Bauer,G. (2009) Preintegration HIV-1 inhibition by a combination lentiviral vector containing a chimeric TRIM5 alpha protein, a CCR5 shRNA, and a TAR decoy. *Mol. Ther.*, **17**, 2103–2114.
44. Schubert,S., Gül,D.C., Grunert,H.P., Zeichhardt,H., Erdmann,V.A. and Kurreck,J. (2003) RNA cleaving '10-23' DNAzymes with enhanced stability and activity. *Nucleic Acids Res.*, **31**, 5982–5992.
45. Jakobsen,M.R., Haasnoot,J., Wengel,J., Berkhout,B. and Kjems,J. (2007) Efficient inhibition of HIV-1 expression by LNA modified antisense oligonucleotides and DNAzymes targeted to functionally selected binding sites. *Retrovirology*, **4**, 29.
46. van den Haute,C., Eggermont,K., Nuttin,B., Debyser,Z. and Baekelandt,V. (2003) Lentiviral vector-mediated delivery of short hairpin RNA results in persistent knockdown of gene expression in mouse brain. *Hum. Gene. Ther.*, **14**, 1799–1807.
47. ter Brake,O. and Berkhout,B. (2007) Lentiviral vectors that carry anti-HIV shRNAs: problems and solutions. *J. Gene Med.*, **9**, 743–750.